

Accepted Manuscript

Freezing of aqueous solutions and chemical stability of amorphous pharmaceuticals:
water clusters hypothesis

Evgenyi Shalaev, Alan Soper, J Axel Zeitler, Satoshi Ohtake, Christopher J. Roberts,
Michael J. Pikal, Ke Wu, Elena Boldyreva

PII: S0022-3549(18)30453-2

DOI: [10.1016/j.xphs.2018.07.018](https://doi.org/10.1016/j.xphs.2018.07.018)

Reference: XPHS 1230

To appear in: *Journal of Pharmaceutical Sciences*

Received Date: 8 May 2018

Revised Date: 13 July 2018

Accepted Date: 17 July 2018

Please cite this article as: Shalaev E, Soper A, Zeitler JA, Ohtake S, Roberts CJ, Pikal MJ, Wu K, Boldyreva E, Freezing of aqueous solutions and chemical stability of amorphous pharmaceuticals: water clusters hypothesis, *Journal of Pharmaceutical Sciences* (2018), doi: 10.1016/j.xphs.2018.07.018.

This is a PDF file of an unedited manuscript that has been accepted for publication. As a service to our customers we are providing this early version of the manuscript. The manuscript will undergo copyediting, typesetting, and review of the resulting proof before it is published in its final form. Please note that during the production process errors may be discovered which could affect the content, and all legal disclaimers that apply to the journal pertain.



Freezing of aqueous solutions and chemical stability of amorphous pharmaceuticals: water clusters hypothesis

Evgenyi Shalaev¹, Alan Soper,² J Axel Zeitler³, Satoshi Ohtake,⁴ Christopher J Roberts,⁵ Michael J Pikal,⁶ Ke Wu,¹ Elena Boldyreva^{7,8}

¹Pharmaceutical Development, Allergan plc, Irvine, CA 92612, USA

²ISIS Facility, STFC Rutherford Appleton Laboratory, Harwell Campus, Didcot, Oxon OX11 0QX, United Kingdom

³Department of Chemical Engineering and Biotechnology, University of Cambridge, Philippa Fawcett Drive, Cambridge CB3 0AS.

⁴Pfizer BioTherapeutics Pharmaceutical Sciences, Chesterfield, MO, USA

⁵Department of Chemical Engineering, University of Delaware, Newark, DE 19716, USA

⁶Department of Pharmaceutical Sciences, School of Pharmacy, University of Connecticut, Storrs, Connecticut, CT 06269 USA

⁷Novosibirsk State University, Pirogova Street 2, Novosibirsk, 630090, Russian Federation

⁸Boreskov Institute of Catalysis SB RAS, Novosibirsk, 630090, Russian Federation

Abstract.

Molecular mobility has been traditionally invoked to explain physical and chemical stability of diverse pharmaceutical systems. While the molecular mobility concept has been credited with creating a scientific basis for stabilization of amorphous pharmaceuticals and biopharmaceuticals, it has become increasingly clear that this approach represents only a partial description of the underlying fundamental principles. An additional mechanism is proposed herein to address two key questions: (1) the existence of unfrozen water (i.e., partial or complete freezing inhibition) in aqueous solutions at subzero temperatures, and (2) the role of water in the chemical stability of amorphous pharmaceuticals. These apparently distant phenomena are linked *via* the concept of water clusters. In particular, freezing inhibition is associated with the confinement of water clusters in a solidified matrix of an amorphous solute, with nanoscaled water clusters being observed in aqueous glasses using wide-angle neutron scattering. The chemical instability is suggested to be directly related to the catalysis of proton transfer by water clusters, considering that proton transfer is the key elemental reaction in many chemical processes, including such common reactions as hydrolysis and deamidation.

I. Introduction.

Amorphous solid (glassy) states are ubiquitous in both nature and industrial products. For example, small molecular weight drugs are commonly formulated with amorphous polymers in order to improve apparent solubility and bioavailability, whereas protein molecules are usually embedded in a freeze-dried amorphous sugar matrix to improve stability and shelf life. In frozen biopharmaceuticals, such as viral vaccines and gene delivery vectors, the active ingredients are present in an amorphous freeze-concentrated fraction which coexists with ice crystals. It is not surprising, therefore, that amorphous solids have been extensively studied. In the past, the majority of efforts were devoted to assess the mobility of amorphous pharmaceuticals, with the glass transition attracting most of the attention.¹⁻⁴ Such initial emphasis on molecular mobility and glass transition was indeed very natural, considering that the most dramatic and obvious result of liquid-to-glass conversion is the increase in viscosity by many orders of magnitude in a relatively narrow temperature interval. In addition, the glass transition temperature (T_g) can be conveniently measured using common laboratory instruments. More recently, studies of the molecular mobility in aqueous glasses were extended beyond the T_g and alpha-relaxation, to include fast and less-cooperative mobility modes, in particular Johari-Goldstein beta-relaxation.⁵⁻⁸ A comprehensive picture of the molecular mobility landscape is emerging, with the potential energy surface (PES) introduced in order to describe both the intra- and inter-molecular features of disordered solids.⁹ A potential practical utility of the PES has also been demonstrated, by using high-powered terahertz pulses to induce crystallization and preferential growth of crystalline polymorphs in glasses. It has been increasingly clear, however, that relationships between molecular mobility and certain properties of the pharmaceutical glasses (e.g., chemical stability) are not straightforward. As an implicit recognition of the fact that mobility alone is not sufficient for a comprehensive description of amorphous materials, the subject of structure has recently attracted the attention of the pharmaceutical science community.¹⁰⁻¹⁴ In particular, the heterogeneous nature of amorphous solids, which are proposed to consist of domains with local (short-range) order resembling local arrangements in the crystal lattice, has been emphasized.^{11,14} The loss of the long-range order between the domains is caused by the lack of translational and rotational coordination of molecules belonging to different domains. The origin of this domain-structure concept is probably related to the Adam-Gibbs theory¹⁵ of cooperatively rearranging clusters, with the heterogeneity length scale corresponding to the cluster size.

Despite the recent interest in amorphous structure, the “molecular mobility” concept is still dominant in the majority of discussions in the field of amorphous pharmaceuticals. In particular, two important phenomena, i.e., (a) the existence of unfrozen water in aqueous solutions at subzero temperatures, and (b) the impact of water on the stability of amorphous pharmaceuticals, are usually considered to be directly related to molecular mobility. Popular viewpoints among pharmaceutical scientists on these two subjects can be expressed as follows:

- (1) Unfrozen water, which is common in aqueous solutions of sugars, organic polymers, and other amorphous solutes, exists because of a greatly reduced molecular mobility associated with the transformation of the freeze-concentrated solution to the glassy state;
- (2) Increase in the water content in an amorphous product negatively impacts the stability due to enhanced mobility.

While these viewpoints in the role of molecular mobility are intuitive and provide an easy way to explain both incomplete freezing and destabilization of amorphous (e.g. freeze-dried) materials by water, they are nevertheless oversimplified and are not necessarily supported by experimental observations.

The first statement was historically based on the Stokes–Einstein (SE) equation, which connects diffusion coefficient with viscosity. However, it is also known that there is a breakdown in the SE relationship for high-viscosity systems, with the diffusion coefficient becoming partially decoupled from viscosity in the vicinity of the T_g .¹⁶⁻²⁰ Moreover, there are direct experimental observations of decoupling of water mobility from that of the matrix and relatively fast diffusion of water well below the T_g , as will be discussed in this paper in some details. An additional mechanism to address the “unfrozen water” question is therefore explored, which is based on the recent neutron scattering studies of water structure^{21,22} while also taking into account the dynamic properties of concentrated aqueous solutions and glasses. Specifically, it is proposed that the incomplete water-to-ice transformation is directly caused by the confinement of water in a solidified matrix created by the solute molecules below the T_g . In order to address the role of water in chemical instability of amorphous solids (i.e., the second statement above), mechanistic details of the chemical processes are considered by utilizing the knowledge accumulated over many years in solution chemistry. In particular, the water clustering concept is used to link the structural organization of water in glasses with the critical elementary reaction step in many chemical processes, that is, proton transfer.

II. Freezing of aqueous solutions with amorphous solute: water confinement.

II.1. Water mobility and the freezing behavior of aqueous solutions.

Freezing (water-to-ice conversion) in aqueous solutions with amorphous solutes, e.g., many polyhydroxy compounds (PHC) and organic polymers, is usually incomplete, although the extent of the retention of the unfrozen water depends on the concentration and properties of a solute. In relatively dilute solutions, hexagonal ice coexists with the freeze-concentrated fraction consisting of the solute and unfrozen water, with the water content in the freeze concentrate ranging typically from approximately 30 to 15 wt%.^{23,24} In solutions with a high concentration of a solute (e.g., above 70 wt% for PHC-water systems), ice does not form at all, and the system remains in a supercooled single-phase amorphous state. As a typical example, **Figure 1** shows differential thermal analysis (DTA) curves of sucrose-water mixtures with water concentration ranging from 40 to 23 wt% (60 to 77 wt% sucrose).²⁵ The DTA curves show ice forming during cooling of solutions with sucrose concentration of $\leq 62.5\%$ (water content $\geq 37.5\%$), whereas the 77 wt% sucrose solution remained completely amorphous during cooling and subsequent heating. The most interesting behavior is exhibited by 65% sucrose solution, which remained amorphous after cooling, whereas the heating curve showed the glass transition immediately followed by the crystallization exotherm. The exotherm is due to water crystallization (ice formation). It was also shown that in concentrated sucrose solutions the exotherm corresponds to the formation of cubic ice, which converted into the hexagonal ice upon further heating. The example in **Figure 1** demonstrates that (i) there is a threshold concentration of a solute above which ice formation is prevented, and (ii) when ice is formed during heating, the water crystallization takes place shortly after the sample is heated above the T_g , thus linking water-to-ice conversion with the T_g .

Concentrated solutions of sorbitol²⁶ and a number of other solutes (e.g., glycerol, glucose,²⁷ polyvinylpyrrolidone (PVP),^{28,29} proteins³⁰) exhibited similar behavior, although an exact concentration threshold for inhibition of ice formation can depend on the chemical nature of the solute as well as on the experimental conditions, in particular on the cooling rate. The type of behavior which is exemplified by the 65% sucrose (i.e., crystallization of water after heating above the T_g , **Figure 1**) is probably the main reason why the inhibition of freezing by various noncrystalline solutes (including PHC) was considered to be a purely kinetic phenomenon, due to a steep increase in viscosity as the supercooled solution transforms to the glassy state during cooling. According to this view (which was also supported by one of the authors of this paper), water diffusion and therefore its crystallization was expected to be prevented below the glass transition temperature, T_g , of the system.^{31,32} During heating, it was argued, as the system converts from glass to supercooled liquid (endothermic step T_g , **Figure 1**), water diffusion is no longer inhibited, and therefore crystallization commences (e.g., the exotherm, water crystallization, in **Figure 1**). This description is consistent with the thermal analysis data, but the underlying assumption of the direct connection between the calorimetric T_g and water diffusion, i.e., that the water diffusion essentially stops below the T_g on the experimental time scale, is not correct. One simple example of water diffusion on a laboratory time scale in systems below the T_g of the system is the common practice to absorb/desorb water into/from a glassy solid by exposure to a series of relative humidities to develop a water sorption/desorption isotherm.

Relations between viscosity, diffusion, glass transition, and crystallization are not straightforward. While diffusion coefficient is inversely proportional to the viscosity for non-viscous liquid, as described by the SE equation, the SE relation is no longer valid for highly viscous systems. The break for the SE equation was reported to occur above their calorimetric glass transition temperatures.¹⁶ In PHC–water mixtures, in particular, the break in the SE relationship was observed at $1.16T_g$ for the diffusion of fluorescein in water–sucrose mixtures,¹⁷ at $1.32T_g$ for ferrocene–methanol diffusion in sucrose–water solutions,¹⁸ at $1.5T_g$ for glycerol and $1.53T_g$ for ferrocene–methanol diffusion in water–glycerol, and at $1.67T_g$ for fluorescein diffusion in trehalose–water.¹⁹ For diffusion of water in a PHC–water solution, the break in the SE relationship was reported at $1.25T_g$.²⁰ Furthermore, while a major decrease in the probability of crystallization below the T_g was observed in various systems ranging from small molecules^{13,33,34} to model biological membranes,³⁵ the inhibition of crystallization below T_g is not a universal phenomenon, and crystallization (both nucleation and crystal growth) was reported to occur below the T_g , albeit at a slower rate.³⁴

Furthermore, translational diffusion of water does not stop on the experimental time scale even well below the T_g . Water diffusion coefficient in several glasses was determined to be between 10^{-9} to 10^{-12} cm²/s, depending on the composition of the system (in particular water content) and measurement technique.³⁶ Zhu et al.³⁷ employed Raman microscopy with D₂O/H₂O exchange, as well as nuclear magnetic resonance (NMR), to determine the self-diffusion coefficient of water in a maltose glass at various water contents. The Raman experiments covered a wide range of water contents of approx. 15 to 4 wt%, corresponding to T_g values ranging from 250 to 330 K (the diffusion measurements were performed at 296 K). While water diffusion slowed down through reduction in water content, no break in the dependence of diffusion coefficient versus water content around T_g was observed. Water diffusion was found to be decoupled from maltose diffusion. The estimated value of the diffusion coefficient of carbohydrate (D_c) at T_g is 10^{-16} cm²/s, whereas the water diffusion

coefficient (D_w) at the same water content (i.e., 8 wt %) is approximately 10^{-10} cm²/s. Thus at T_g , $D_w/D_c = 10^6$, whereas at higher water contents, D_w/D_c was found to be approximately 10. Even higher values of the water diffusion coefficient were reported for sucrose-based materials ($0.5 \cdot 10^{-9}$ to $4 \cdot 10^{-9}$ cm²/s)³⁸ and for several polymers in the glassy state ($2.4 \cdot 10^{-9}$ to $3 \cdot 10^{-8}$ cm²/s).³⁹

Decoupling of the mobility of water molecules from that of the matrix was reported for amorphous sucrose and sorbitol systems based on NMR⁴⁰ and thermally stimulated current (TSC) experiments.²⁶ In the TSC study, in particular, a dipole relaxation peak, which was marked as T_{gw} in the original publication, was observed in amorphous sucrose and sorbitol between -125 and -155°C at water contents of 35 to 1 wt%. The T_{gw} temperatures in both systems were found to be similar to the T_g values reported for the amorphous ice, that is, -137°C to -149°C.⁴¹⁻⁴⁴ This observation of the similarity of the T_g in amorphous ice and in sorbitol-water glasses is consistent with a wide-angle neutron diffraction study, which is described in the next section in some details. The neutron diffraction study demonstrated that the structure of water clusters in 70 wt % sorbitol solution is similar to that of low-density amorphous ice (LDA), but different from bulk water.²² The T_{gw} is apparently independent of the sugar type, as both sucrose and sorbitol samples furnished similar T_{gw} values at comparable water contents. The strength of the T_{gw} event was much stronger in samples with higher water content (23-30 wt%) than in amorphous sucrose samples with low water content (1 to 5 wt%). It was concluded that the T_{gw} corresponds to the onset of dipole relaxation of water in sorbitol and sucrose glasses, most likely to a reorientation of hydrogen bond network involving rotational mobility of water molecules. In addition, the terahertz (THz) spectroscopy study of the 70 wt% sorbitol solution showed a transition from a state with predominantly vibrational mobility modes to one with rotational mobility at approximately 160 K (-113°C).⁴⁵ The decoupling between the T_g of the matrix and mobility of water is illustrated in the solid-liquid state diagram for a binary solute-water system (the low-temperature part of the diagram is presented in **Figure 2**), which combines both the calorimetric T_g of the matrix and the characteristic temperatures for water mobility, including the ideal glass transition temperatures for sucrose-water system measured by NMR, and the TSC-detected T_{gw} events. In addition, transitions observed by THz spectroscopy in amorphous sorbitol and sorbitol-water mixture, and the low-temperature glass transition in Nafion-water system (which is discussed later) are also shown.

We shall also point out the well-known observation, which by itself would raise major doubts about any attempts to defend the idea about “immobile water below the T_g ”, as follows: water is readily removed from solid amorphous materials (i.e., below the T_g) during freeze-drying. This observation has been reproduced on countless occasions in numerous freeze-drying laboratories and manufacturing sites. Indeed, the residual water content in the majority of freeze-dried materials is typically 0 to 3 wt%, and achieving this water content would be impossible if water was immobile below the T_g . While the T_g values for freeze-dried pharmaceuticals could be as low as around 50°C (sucrose-based formulations), they are typically much higher and can reach 150°C and above for polymer- and protein-rich formulations. In addition, there are direct case studies, which demonstrate relatively fast drying of amorphous materials well below the T_g . As an example, removal of water from an amorphous material, PVP, during secondary drying was studied⁴⁶; in this case, the T_g (T_g of PVP K-90 is > 70°C at water content ~ 6 wt%⁴⁷) was much higher than the drying temperature of 2 and 18°C. Moreover, a substantial portion of the unfrozen water can also be removed during the primary drying segment, which is performed at sub-zero temperatures, typically below -20°C. For

example, during primary drying of a sucrose solution,⁴⁸ water content was reduced from 25% (which is slightly higher than the water content in the maximally freeze-concentrated solution) to less than 5% within a few hours, indicating a fast diffusion of water molecules at $T_g - T > 45^\circ\text{C}$ (sample temperature during drying was $< -15^\circ\text{C}$, and the T_g of sucrose with 5% water is $\sim 30^\circ\text{C}$).

Overall, the evidence of significant water mobility below the T_g of the glass-forming matrix is overwhelming, and therefore the “ T_g /molecular mobility” explanation of the inhibited (in concentrated solutions) or incomplete (in dilute solutions) water-to-ice transition is oversimplified and not entirely satisfactory. Two additional mechanisms to supplement the “molecular mobility/vitrification” concept in respect of freezing behavior are introduced here as follows. The first hypothesis is based on the fact that the specific volume of ice is higher than that of the liquid water. The density of liquid water is almost 10% higher than that of ice,⁴⁹ and water-to-ice transformation results in a corresponding volume expansion. At the start of freezing, an ice crystal would have an opportunity to grow and expand without restrictions, while the room for the expansion would be more limited by the time the majority of water has transformed to ice. In the later stage of freezing, ice crystals will encounter greater resistance for growth from neighboring crystals and the rigid (glassy) freeze concentrate fraction, resulting in increased mechanical stresses and local pressure build-up. It was suggested, for example, that such freezing-related expansion could create significant mechanical stresses equivalent to local hydrostatic pressure of 2-3 kBar.⁵⁰ Critically, such increase in pressure rise would reduce the melting point of hexagonal ice (Ih), up to 250K at 2 kBar.⁵¹ Therefore, the volume expansion could, at least in principle, greatly reduce or even eliminate the thermodynamic driving force for water-to-ice transformation. Note also that the elevated pressure and shear stresses, which are created by growing ice crystals, could lead to destabilization of protein molecules during freezing. Interestingly, an inhibition of ice formation by freezing-created pressure was recently put into practice in evaluation of cold-induced destabilization of proteins.⁵²

Another explanation for the existence of unfrozen water was suggested in a recent study,²² in which the suppression of water-to-ice transformation was attributed to the combination of confinement of water and the glass transition of the matrix. Coincidentally, a somewhat similar hypothesis (although not explicitly expressed in terms of confinement) was proposed more than 20 years ago to explain the existence of unfrozen water in proteins.⁵³ Since then, the impact of confinement on the freezing behavior has been studied extensively. It has been shown, in particular, that when water is absorbed in MCM-41 (Mobil Composition of Matter No. 41) or other typical mesoporous materials of small pore size, it can be supercooled below the homogeneous ice nucleation temperature. Furthermore, water crystallization (ice formation) can be completely avoided if the pore size is smaller than a certain threshold value. In addition, ice melting temperature depends on the pore size as described by the Gibbs-Thompson equation: the smaller pore – the lower melting temperature. **Figure 3** shows the experimentally-determined depression of the freezing point and ice melting temperature as a function of the pore size.⁵⁴ Note also that there is another similarity in the freezing behavior between water in nanopores and sugar solutions, that is, formation of cubic ice, which was reported in both confined water⁵⁵ and concentrated solutions of various solutes. For example, cubic ice was reported to form in solutions of sucrose,²⁵ glucose,⁵⁶ and other solutes.⁵⁷

As described in the next section, water structure in a model polyhydroxy compound-water mixture, 70% sorbitol-30% water, was related to that of water confined in a solid porous silicate material, MCM-41, which has a well-defined pore size and structure and been extensively studied.⁵⁸⁻⁶³

11.2. Water confinement in amorphous sorbitol.

In this section, water structure in 70% sorbitol – 30% water is compared with the structure of water in a well-defined solid confinement in MCM-41.²² The results are based on the wide-angle neutron scattering data, which were interpreted in terms of a molecular structure model, using empirical potential structure refinement (EPSR). It was shown that the sorbitol-water mixture is heterogeneous on a sub-nanometer lengthscale, consisting of water-filled voids in a sorbitol matrix. The simulation box is shown in **Figure 4a** to illustrate the presence of pores (voids) in the sorbitol matrix, which are filled by water (water molecules are not shown). In order to estimate the corresponding lengthscale of the water-filled areas in the sorbitol matrix, the volume distribution function was obtained for water in 70 wt % sorbitol at two temperatures, 100 and 298 K (**Figure 4c**). The volume distribution functions at 298 and 100 K are essentially identical. The asymptotic behavior at large distances (large r) of these functions represents the volume fraction of water in the solution, which is about 40% at this concentration. The low r behavior of this function is a measure of the “confining distance” of water, which in this case is quite small, approximately 5.0 Å (tangent line shown in blue in **Figure 4c**). Note that this distance, although expressed as diameter, cannot be interpreted as implying that the pores are necessarily spherical in shape. The characteristic size of the water region in the 70% sorbitol-water sample is marked with the arrow in **Figure 3**, showing that the dimensions of water areas in sorbitol matrix are much smaller than the threshold value associated with inhibition of freezing. In particular, the melting temperature depression for 5 Å pores could exceed 100 K, based on the extrapolation of the melting point depression line in **Figure 3**. Therefore, water confined in the solid sorbitol matrix is expected to be thermodynamically stable in the liquid state at temperatures as low as 130 K (the equilibrium melting point for 70% sorbitol is approximately 230 K, as estimated from the water liquidus).

To visualize water-occupied regions, **Figure 4b** shows a surface contour of water density in the 70 wt% sorbitol–water system at 100 K. The surface contour of water density demonstrates that water occupies a predominantly percolating volume in this solution, with only occasional isolated water molecules.

Local structure of water in sorbitol was compared with water in MCM41 and the ordinary (bulk) water, using atomic radial distribution functions (RDFs). Water oxygen-oxygen (OW-OW) RDFs at 298 K are provided in **Figure 5a**. The first peak and the minimum after the first peak represent the first coordination sphere, the second peak is due to the second coordination sphere, and so on. Positions of the peaks correspond to the average distances between oxygens in water molecules in the first, second, etc. coordination spheres, whereas the width of the peak reflects the distribution of the distances. The higher intensity of the first peaks in the radial distribution functions for both MCM-41-water and sorbitol-water compared to bulk water reinforces the idea that the water is not uniformly distributed in the sorbitol matrix. The degree of sharpness (ordering) of the first coordination shell for water between the three systems was compared using the full width at half-maximum (FWHM). The FWHM for the first peak in OW-OW $g(r)$ s are plotted in **Figure 5b**. The FWHM values for water in both MCM-41 and sorbitol matrices are lower than for the bulk water at

298 K, indicative of a narrower distribution of the distances in the first shell in these systems. The FWHM value for water in MCM-41 is higher than that for water in sorbitol at 298 K, whereas they become essentially identical after cooling to approximately 210 K. Interestingly, the ordering of the first coordination sphere (as reflected in the FWHM) in sorbitol is similar to that for Ih, indicative of the similar degree of order in the first OW-OW coordination sphere on the sub-nm lengthscale. Whereas the longer-range order is very different between crystalline ice (multiple peaks in the RDF indicative of the highly ordered structure, blue curve in **Figure 5a**) and water in the amorphous sorbitol-water system (only 3 peaks corresponding to the first, second, and third coordination spheres, black curve in **Figure 5a**), as expected.

In addition to the translational order, orientational order of water molecules was also studied, by analyzing the region around the second peak in the OW-OW $g(r)$, which reflects the tetrahedral arrangement of water molecules. At 298 K, $g(r)$ for water in sorbitol exhibited two poorly resolved peaks, in contrast to water in MCM-41 with a single peak (**Figure 5a**). This is interpreted as a difference in the tetrahedrality of water in MCM-41 vs water in sorbitol, at least at 298 K. Cooling the system to 213 K, however, resulted in a noticeable change in the shape of the second peak, as highlighted in **Figure 6b**, which shows a magnified portion of the $g(r)$ region around the second peak. While the 298 K pattern had two poorly resolved peaks at r values of 2–5 Å, cooling from 298 to 213 K produced a single peak with a shoulder, indicative of a change in the tetrahedral arrangement of water molecules. At 213 K, the $g(r)$ pattern in the second peak region became similar to that for water in MCM-41 at 210 K (**Figure 6c**). This modification of the orientational order took place slightly above the T_g ($T_g \sim 200$ K). Further cooling to 173 K and finally to 100 K did not introduce any additional changes in the $g(r)$ patterns (**Figure 6b**).

Additional (and more quantitative) information on the orientational structure of water was obtained using the OW-OW-OW triangles distributions, and from a tetrahedrality parameter, q . The q order parameter was introduced by Errington and Debenedetti⁶⁴ and was redefined for aqueous systems.²¹ The OW-OW-OW triangle distributions at four temperatures are represented in **Figure 7a**, and the corresponding values of q are provided in **Figure 7b**. All four triangle distributions (**Figure 7a**) show a broad peak at approximately 100° corresponding to loosely tetrahedrally bonded arrangements of triplets of neighboring water oxygen atoms, plus a peak near 60° corresponding to triplets for which at least one pair of the hydrogen bonds is heavily distorted or broken. There is an obvious difference in the tetrahedral peak between 298 K and lower temperatures of 213 to 100 K, with the lower temperature patterns showing a stronger tetrahedral arrangement. At 213 K, the peak was centered at approximately 109.5°, closely corresponding to the ideal tetrahedral angle of 109.47°, whereas at 298 K a flat hump (rather than a peak) was observed between approximately 80° and 120°. Accordingly, the temperature dependence of the q parameter showed a marked increase (i.e., increase in the tetrahedrality) upon cooling from 298 to 213 K, whereas the q was essentially constant between 213 and 100 K (**Figure 7b**). Furthermore, the tetrahedrality of water in the sorbitol matrix is compared with the q parameter in bulk water and water confined in MCM-41. The q parameter at 298 K is different between all three systems, probably due to the influence of the surrounding (i.e., bulk water vs water in solid pores of MCM-41 vs water in the mobile matrix of sorbitol). Upon cooling to 210 K, the q value for water confined in the MCM-41 approaches the value for water in sorbitol. As also shown in **Figure 7b**, the calorimetric glass transition temperature of 70%

sorbitol is approximately 200 K, i.e., below the temperature range in which the increase in the tetrahedral structure of water was observed (between 298 and 213 K).

Overall, the similarity in the local ordering of water molecules in sorbitol vs confined water in MCM-41, combined with the small (5 Å) size of the water region in sorbitol matrix (see **Figure 4c** and corresponding text), provides a strong support for the “freezing inhibition is due to the confinement of water in a sugar matrix” hypothesis. It should be mentioned, however, that additional factors might also contribute to the inhibition of freezing. For example, connectivity between water areas might also be relevant to the freezing inhibition. When water content decreases below a percolation threshold value, water regions become isolated from each other. For glucose-water system, for example, the percolation threshold was estimated to be 18 wt % water,⁶⁵ whereas a loss of a percolating network of water–water hydrogen bonds was reported to occur at a higher water content of approximately 40 wt% in several sugar-water systems (alpha-D-glucose, alpha-D-mannose, and D-fructose).⁶⁶ A lower percolation threshold was observed for glycerol-water system, with the threshold value between 0.8 and 0.5 glycerol fraction (4.7 to 17.4 wt% water).⁶⁷ Based on this brief discussion, a comprehensive explanation of freezing inhibition might require a third component (i.e., water percolation threshold), in addition to confined water clusters and solidification of the matrix’s walls below the T_g . Note also that the hypothesis on freezing inhibition, as presented in this paper for PHC-water systems, might not be universal, and other types of systems could be governed by different mechanisms. For example, the break of the tetrahedral structures was reported in studies of water and aqueous salt solutions under pressure. It was therefore suggested that the repression of water crystallization could be due to the disruption of the orientational order (tetrahedral structures) from which ice Ih nuclei could form.^{68,69} It is possible that the behavior of ionic systems could be different from that of the sorbitol-water system, for which tetrahedrality freezing is inhibited without disruption of tetrahedrality. Considering that the absolute majority of pharmaceutical formulations contain salts and other ionic species, a study to compare water structure in aqueous solutions of ionic solutes vs PHC solutions would be warranted.

II.3. Summary: Water structure in soft confinement and freezing.

In order to explain the inhibited (in concentrated aqueous solutions) or incomplete (in dilute solutions) water-to-ice transition, a novel hypothesis has been proposed, which combines thermodynamics and kinetics mechanisms. The key elements of the hypothesis, which is formulated using concentrated sorbitol - water solution as a representative example, are as follows:

- (i) Sorbitol creates a matrix with voids of sub-nm size, which are filled by water;
- (ii) The sorbitol matrix solidifies when the temperature approaches the T_g . At this point, the system resembles a mesoporous material with solid pores filled with water.
- (iii) Water, which is confined in the solid pores, does not freeze, due to the size-dependent melting point depression (**Figure 3**).

The following description of the cooling process in a concentrated sorbitol-water solution is therefore proposed. At room temperature, water clusters, which occupy voids in the sorbitol matrix, have their mobility coupled with that of the matrix. Upon cooling to a temperature close to the T_g , the tetrahedral structure of water is enhanced and becomes similar to water confined in MCM-41 pores with solid walls. Simultaneously, the macroscopic viscosity increases dramatically, and mobility of water molecules becomes uncoupled from the viscosity; e.g., water diffusion is no longer

described by the Stokes–Einstein relationship. At this point, the walls of voids in the sorbitol matrix, as “seen” by water molecules, solidify and resemble those in solid pores in MCM-41 or other solid porous material. Considering that water in pores does not freeze when the pore diameter reaches a critical value of approximately 2 nm,⁵⁴ it is proposed that the prevention of ice formation in 70 wt % sorbitol–water solution is due to the confinement of water in the solidified sorbitol matrix.

III. Role of water in chemical reactivity of organic glasses: proton transfer and water clusters.

III.1. Water as a plasticizer vs catalyst in chemical reactivity: overview.

Water is the most ubiquitous plasticizer; therefore, it is easy to understand the common belief (among pharmaceutical scientists) in the following sequence: increase in the water content in an amorphous product enhances mobility, which in turn causes decrease in stability. The “water → mobility → instability” concept is very attractive, especially for applied scientists, because it is intuitive and easy to explain. Also, the T_g and other mobility-related properties (e.g., global relaxation time) are routinely measured experimentally, and therefore can be conveniently embedded into drug product development process. Nevertheless, this concept fails to describe certain experimental observations of complicated relationships between water content and stability.

In an early attempt to provide a more systematic overview of different mechanisms by which water could impact chemical stability, the “water as a plasticizer” hypothesis was tested *via* a semi-quantitative estimation of an impact of water on the rate of a diffusion-controlled reaction.⁷⁰ Two hypothetical systems (a strong and a fragile glass former) were considered.⁷⁰ It was shown that the increase in water content by only a few percent could accelerate a diffusion-limited reaction by several orders of magnitude through its plasticizing effects. In addition, this “water as a plasticizer” effect can be quite different depending on the fragility of a particular system: the more fragile the system, the greater the effect of water on the reaction rate. Even in the most conservative scenario considered (strong glass former and a partial decoupling between mobility and reactivity), the rate of reaction was predicted to increase by almost 500x as water content increases from 0 to 3 wt%; moreover, in a more fragile (and more common) system, the reaction could be expected to accelerate by 14 orders of magnitude! Such dramatic changes in the reaction rates with a very modest change in water content have been rarely (if ever) observed experimentally. These simple estimations, along with more recent experimental studies showing rather weak correlations between alpha relaxation (structural relaxation) and chemical stability,^{71,72} provided a powerful motivation to explore alternative mechanisms for the role of water in solid-state amorphous chemical reactivity.

In recent reviews, the role of water in the chemical instability of amorphous materials was reconsidered, with the focus on the amide hydrolysis and deamidation reactions.^{73,74} The analysis of several case studies enabled the authors to highlight two probable mechanisms, that is, water as plasticizer/antiplasticizer of local mobility and fast relaxation modes (as previously proposed by Cicerone et al.^{7,8}) and water as a reaction medium, in particular, in water-supported proton transfer. It was also noted that for proteins, which possess higher-order structure, water could play a dual role as both a destabilizer, *via* water catalysis, and a stabilizer of protein native structure (role of water in the maintenance of protein higher-level structure was reviewed elsewhere⁷⁵). It was concluded^{73,74}

that the hydrolysis and other relevant reactions in the amorphous solid state are under chemical (rather than diffusion) control (e.g., for amide hydrolysis in zoniporide³⁸), and that global alpha relaxation is probably not a chemical stability-defining factor in these systems. This conclusion is consistent with the emerging view that reactions that do not require whole molecule diffusion (i.e., motion over long length scales) are essentially uncoupled from structural relaxation dynamics.⁷⁶

In order to illustrate the fact that impact of water can be entirely described by chemical mechanisms, without invoking any molecular mobility considerations, **Figure 8** provides several examples, which demonstrate change in the reaction rate vs water content for solution reactions. The same figure shows the impact of water on the chemical instability in amorphous freeze-dried materials. It can be seen that the change in the reaction rate with water content in amorphous freeze-dried materials is in the same range as that observed in solution reactions.

To summarize, there are multiple reasons to consider the role of water beyond the molecular mobility explanation; examples of such reasons include: (1) the observation of similar magnitudes of the impact of water between reactions in solutions and amorphous solids (**Figure 8**), (2) chemical (not diffusion) control of hydrolysis reaction in a freeze-dried formulation,³⁸ (3) weak correlations between structural relaxation rate and chemical reactivity in many amorphous solids,⁷² and (4) the established catalytic role of water in various heterogeneous chemical reactions.⁷⁷ Therefore, it would be logical to extend the knowledge, acquired in numerous studies on the chemical mechanisms of the role of water in various systems, to amorphous solids, as described in the next two sections.

III.2. Water catalysis and proton transfer.

One of the most prominent features of water molecules, as far as various chemical processes are concerned, is their ability to catalyze proton transfer reaction. Proton transfer is the first step in numerous chemical processes, including such common pharmaceutical degradation reactions as amide hydrolysis and deamidation. In the asparagine (Asn) deamidation reaction in the moderately acidic and basic pH range, for example, a proton is transferred from the backbone NH group in the N+1 residue to the Asn side chain carbonyl group, followed by the formation of the 5-membered tetrahedral intermediate *via* the attack of the backbone nitrogen on the carbonyl carbon.^{78,79} The activation barrier for this reaction was calculated to be 40-50 kcal/mol, which is very high for a solution reaction that occurs readily. Therefore, solvent-assisted mechanism was introduced and evaluated in detail using quantum chemistry calculations.⁷⁹ The participation of water molecules was demonstrated to significantly lower the activation barriers; for example, in one of the pathways explored for the tetrahedral intermediate formation (*via* Asn side chain tautomerization), all water-assisted mechanisms possessed significantly lower activation barriers (by more than 10 kcal/mol) compared to previously proposed waterless, concerted cyclization mechanisms. Involvement of two water molecules resulted in an additional lowering of the activation barrier. Participation of water molecules in the formation of the tetrahedral intermediate is illustrated in **Scheme 1**.⁷⁸ A similar conclusion on the critical role of water molecules in deamidation of asparagine has been reached by Kaliman et al.⁸⁰

A number of relevant chemical processes are also assisted by water. In a computational modeling study of glutamine deamidation, the addition of water molecule was shown to significantly lower the activation barrier by stabilizing the transition state through the creation of a hydrogen bond network

and transfer of proton through water-mediated channels.⁸¹ Isomerization and racemization of aspartic acid in peptides were also reported to be catalyzed by water.⁸² The reaction proceeds *via* a cyclic intermediate, succinimide, and involves a water-assisted quintuple proton transfer along intra- and inter-molecular hydrogen bonds formed by the C-terminal amide group, the side-chain carboxyl group, and critically, three water molecules. The amide hydrolysis reaction also involves water-assisted proton transfer.⁸³ These findings on water catalysis in deamidation and related reactions are consistent with the role of water in many other chemical reactions in solution, as reviewed by Ribe and Wipf.⁸⁴

As a brief summary of water catalysis in solution, water plays the critical role in lowering the activation barrier of many reactions by facilitating proton transfer. In the deamidation reaction, for example, water enables the first reaction step, deprotonation, in which the departing proton from the backbone secondary amine is transferred to a small water cluster nearby. Quantum chemistry studies indicate that the lower activation energies are obtained when the activated complex includes two or more water molecules (i.e., small water clusters), assisting both the amide deprotonation and the stabilization of the zwitterionic transition state.

In order to extend the proton transfer concept to amorphous solids, one should address a question about proton mobility in these materials. In this respect, proton transfer in amorphous solids has been studied by measuring the change in the extent of protonation of probe molecules, sulfonephthalein pH indicators, embedded into the amorphous trehalose-Na citrate matrix.⁸⁵ It was observed that the extent of protonation decreased with the increase in water content, when the freeze-dried material was partially rehydrated *via* water vapor equilibration within several hours. This empirical observation of relatively high proton mobility is consistent with the studies of proton transfer in the liquid state, in which proton hopping (i.e., proton mobility) is uncoupled from both viscosity and water rotation.⁸⁶ Furthermore, H/D exchange experiments provide a direct proof of proton transfer in freeze-dried solids. The level of deuterium incorporation into freeze-dried proteins was found to increase with time approaching a plateau within 24 h of exchange.^{87,88} An indirect support of criticality of proton transfer in solid-state chemical reactivity was obtained in a recent study, in which proton/deuterium exchange in freeze-dried monoclonal antibody (MAB) formulations was compared with the rate of various degradation pathways, including deamidation, oxidation, and aggregation.⁸⁹ It was found that the best correlation was observed with deamidation, the reaction in which proton transfer plays a critical role. Correlation between oxidation rate and H/D exchange, on the other hand, was less obvious. Oxidation, while it also could involve proton transfer,⁹⁰ is by definition electron transfer reaction, and therefore could be partially decoupled from the proton transfer processes.

III.3. Water clusters.

As mentioned in the previous section, water clusters could be expected to be intimately involved in proton transfer reactions as a catalyst. The critical role of water clusters in proton transfer is consistent with the structures of proton in aqueous systems, in which Eigen cation, H_9O_4^+ , and Zundel cation, H_5O_2^+ , serve as the ion core for larger protonated water clusters. As summarized by Eikerling et al.,⁹¹ the proton spends similar amounts of time in the Zundel state H_5O_2^+ as in the Eigen state $\text{H}_9\text{O}_4^+ = (\text{H}_3\text{O})^+3(\text{H}_2\text{O})$, which is the hydrated H_3O^+ ion. In the Zundel state, the excess proton is

delocalized between two water molecules, whereas the proton charge in the Eigen state is largely centered on one oxygen atom and the central H_3O^+ ion is strongly hydrated by three water molecules. Rapid fluctuative interconversions between these two states take place. In fact, “an unambiguous distinction between H_5O_2^+ and H_9O_4^+ can no longer be achieved”.⁹² It was also noted that the equilibrium O – O distance in the Zundel complex is significantly shorter ($r_{\text{OO}} = 2.45 \text{ \AA}$) than the average O – O distance in bulk water (2.85 \AA).⁹¹ The rate of proton transfer between two adjacent water molecules could depend on the H-bond dynamics in the hydration shell of a Zundel cation.⁹³ The disruption of an H-bond in the hydration shell creates the electrostatic conditions for the H^+ to hop between the adjacent oxygens in a Zundel cation. The energy of this H-bond is approximately 2.5 kcal/mol, which is similar to the activation energy of proton mobility in bulk water, in which it takes 1 ps for a proton to move 2.5 \AA distance. The majority of studies on Eigen and Zundel cations were performed in the gas phase⁹⁴ and in aqueous solutions,⁹⁵ whereas observations of these hydrated proton structures in water-related solids (amorphous HCl hydrates⁹⁶ and crystals^{97,98}) were also reported. In organic solvents, on the other hand, it was reported that, while neither Eigen nor Zundel ions were observed, a different form of hydrated proton was present, H_7O_3^+ . The fact that proton exists in predominantly hydrated state and that proton transfers by hopping between adjacent water molecules *via* Grotthuss-like mechanism⁹³ indicates that individual (unclustered) water molecules are probably catalytically less active than water clusters.

Water clusters have been observed in amorphous PHC and polymers using both experiments (WANS and water sorption isotherms) and computer modeling. In a WANS study of glycerol-water mixtures of different concentrations, predominantly non-clustered water molecules were detected at water content of 4.7 wt%, with 56% of water molecules existing as monomers, whereas clusters were found to dominate at 16.4 wt% water.⁶⁷ In another WANS study, water clusters, with characteristic size of approximately 5 \AA , were observed in an amorphous sorbitol matrix (section II.2). A molecular dynamic simulation investigation of amorphous PVP revealed a transition between unclustered to clustered water molecules when water content increased from 0.5 wt% water (unclustered water) to 10 wt% water (water clusters).⁹⁹ The existence of water clusters can also be deduced from the analysis of water sorption data using Zimm’s cluster function, G_{11}/V_1 .¹⁰⁰ For example, water clusters were reported to form in collagen at water volume fraction of approximately 0.35.¹⁰¹ In another water sorption study,¹⁰² small water clusters of average size up to 3.5 water molecules were detected in cellulose and several proteins (collagen, keratin, egg albumin, and serum albumin), albeit at higher relative humidity (RH) values. In egg albumin, for example, clustering occurred at $\text{RH} > 80\%$. Globular proteins (egg albumin and serum albumin) and cellulose formed water clusters at lower RH and lower water contents than fibrillar proteins (collagen and keratin).

While there is little doubt on the existence of water clusters in a range of systems, from pure water to concentrated solutions and nominally dried amorphous solids (see reference¹⁰³ for review), there is a significant discrepancy in the determination of the clustering threshold between different methods. For example, analysis of the water activity (a_w) vs water content data for sorbitol and PVP9000¹⁰⁴, which was performed using a method described in¹⁰⁵, did not show any evidence of water clusters for up to 40 wt% in both systems. In that analysis, the data reported by Peng et al.¹⁰⁶ and MacKenzie and Rasmussen²⁸ were used for sorbitol and PVP, respectively. In addition, based on the analysis of the water sorption data for PVP, water clusters were not observed in PVP at a_w 0.187 – 0.721 at 35°C.³⁹ These findings disagree with the WANS data for sorbitol showing the existence of

water clusters at water content 30 wt%, and MD simulations for PVP, in which water clusters were suggested to form at water content between 0.5 wt% (unclustered water observed) and 10 wt% (water clusters), as discussed above. The apparent contradictions between the conclusions based on the water sorption data vs WANS and MD simulations used to study water clustering remain unexplained, and warrants further investigations.

It would be instructive to compare simple schematic representations of the microstructure of polymer electrolyte membrane and a pharmaceutical glass containing protein and trehalose (**Figure 9**). In both cases, water clusters are shown, although unclustered water molecules are also present. The bottom figure visualizes transition from unclustered water molecules at lower water activities, a_w , to water clusters upon increasing a_w above a certain threshold value.

It should be noted that the concept of a relatively sharp transition between an unclustered region to water clusters should be considered as a hypothesis rather than an established fact. For example, in an ionophoric membrane, Nafion, a significant fraction of water molecules (approximately 20% of the total water molecules) was reported to be unclustered in the entire water content range studied, 3 to 14 wt.% water (i.e., below the water-clustering threshold), based on the deconvolution of the near-infrared (NIR) peak using the three-state model (water molecules with 0, 1, and 2 H-bonds).¹⁰⁷ Whether such co-existence of water clusters with unclustered water molecules in a wide range of water content is also relevant to pharmaceutically representative materials, such as PHC, remains to be seen.

The critical role of water clusters as the media for proton transfer has been invoked to explain experimentally observed kinetic curves (original data reported in ¹⁰⁸⁻¹¹⁰) for chemical degradation *via* deamidation of several freeze-dried proteins.⁷⁴ In these cases, the deamidation rate constants were essentially independent of water in the lower water content range,^{108,109} whereas the reaction accelerates upon increasing water content above a threshold.¹¹⁰ An example of such “hockey stick-type” relationship between degradation rate and water content is presented in **Figure 10**, which also shows the treatment of the experimental data using a “water content threshold” model. Within this model, individual (unclustered) water molecules, that are prevalent in freeze-dried solids at lower water contents, are considered to be catalytically less active in comparison to water clusters. Acceleration of deamidation reaction at higher water contents was attributed to the formation of water clusters which facilitate the proton transfer.⁷⁴ It should be noted that there are other possible explanations of the hockey-stick type stability curves. One alternative model to describe the acceleration above certain water content is based on the dual role of water (i.e., both stabilizer of the higher-order structure and destabilizer *via* water catalysis) in the stability of freeze-dried proteins.⁷⁴ Finally, the sharp increase in the deamidation rate (**Figure 10**) coincided with the increase in water content above the W_g value, i.e., water content associated with glass-to-liquid transition, thus leading to quite logical “glass transition” interpretation in the original publication by Breen et al.¹¹⁰ Note, however, that more recent studies point to weak correlations between alpha-relaxation and chemical degradation,^{71,72} thus weakening the mechanistic foundation of the “glass transition” explanation of chemical instabilities. Other degradation processes, such as protein aggregation, are expected to be directly linked with large-scale molecular motions and therefore with the glass transition and alpha-relaxation.

III.4. SUMMARY: water cluster, proton transfer, and amorphous solid-state chemical instability.

It has been proposed that water serves as a catalyst in such common degradation processes as hydrolysis and deamidation, by enabling proton transfer *via* the Grotthuss-like mechanism. Furthermore, the role of water clusters, rather than unclustered water molecules, in the proton transfer is emphasized. Water clusters are formed at water contents above a certain threshold value. At lower water content, water molecules are predominantly unclustered and therefore less catalytically active. It has also been proposed here that, while proton transfer is expected to be decoupled from global mobility, local (fast) non-cooperative processes, such as beta Johari-Goldstein relaxation, might be related to proton transfer and therefore to chemical degradation. The role of the beta-relaxation process in another elementary chemical process, that is, electron solvation reaction, has also been mentioned earlier in an attempt to bridge chemical reactivity with molecular mobility.¹¹¹ Considering that the timescale of proton transfer is in the ps range (at least in solution), it is reasonable to suggest that an experimental tool which measures dynamics on the corresponding scale could be expected to establish correlations between the dynamics (e.g., neutron scattering or THz spectroscopy) and chemical degradation. In addition, measuring H/D exchange, which has been introduced recently as a tool to predict relative stability of freeze-dried proteins,¹¹² can reasonably be expected to be related to proton transfer, and therefore to the rates of such degradation processes as deamidation and hydrolysis.

It should be stressed that the role of water clusters in chemical instability of amorphous pharmaceuticals, as presented here, should be considered as a hypothesis, rather than a proved fact. In order to confirm (or reject) the hypothesis, it would be essential to establish quantitative mechanisms for the role of water clusters in chemical reactions in amorphous solids, which would include addressing multiple questions including:

- (i) Is there a threshold for water clustering, or is there a gradual change in the relative portion of unclustered vs clustered water upon the increase in water content?
- (ii) Do water clusters exist at low water contents that are typical for freeze-dried pharmaceuticals (i.e., less than 5 wt% water)?
- (iii) What are the relationships between water clustering patterns and proton transfer in pharmaceutically relevant amorphous solids, e.g., proteins embedded into sugar glasses?
- (iv) Are there any fundamental chemical mechanisms which could support the hypothesis on relationships between a particular relaxation mode (e.g., as measured by the neutron scattering⁷ or THz spectroscopy¹¹³) and a particular reaction step, e.g., proton transfer in water-mediated deprotonation of amide in deamidation reaction?

Conclusion.

In this paper, such apparently unrelated phenomena as (a) inhibition of freezing in aqueous systems with amorphous solute and (b) water role in chemical reactivity, are linked *via* water clusters. In particular, freezing inhibition is associated with the water confinement in a solidified matrix of an amorphous solute, whereas chemical reactivity is related to the role of water clusters in proton transfer processes. We shall stress, however, that dynamic properties and the role of molecular mobility in freezing and amorphous stability should not be ignored. Indeed, while the molecular

mobility does not stop at T_g , the T_g is probably directly related to inhibition of freezing process, although not in the same way as considered until recently. As proposed in this paper, conversion of the amorphous solute matrix from the liquid to the glassy state solidifies the walls of the water-filled pores, in which water molecules are confined and unable to convert to ice. This solidification of the walls of the “pores” is thought to be an essential component in the freezing inhibition. Furthermore, while we argue that the role of water in chemical reactivity could be connected to water clusters as a proton transfer catalyst, it would be premature to discard the concept that T_g is an important reference point in any stability study. Crystallization, for example, is greatly accelerated above the T_g , and the amorphous-to-crystalline transition can either accelerate degradation of an active ingredient (in cases of crystallization of a lyoprotector), or decrease reaction rate (when amorphous small molecular weight drug is converted into crystalline form). The T_g and global mobility could also be expected to play a major role in processes which require large-scale molecular movement, such as protein aggregation.

The same approach considering the role of water clusters, confinement and proton transfer in physical and chemical stability of amorphous pharmaceutical formulations can prove to be helpful in other fields, e.g., in mechanochemical transformations. Most of the processes on milling and grinding are highly sensitive to the presence of even traces of water. If water is added as fluid phase, one speaks of Liquid Assisted Grinding (LAG). However, it is not solely the amount of water added that matters, but also its state in the system. It has been shown that water released on dehydration of crystal hydrates, sorbed from the atmosphere, confined in the pores of polymeric additives (Polymer Assisted Grinding, POLAG), or in the inter-particle capillary pores can be much more efficient in accelerating the transformation and making it at all possible, than drops of fluid phase. Moreover, this confined water often preserves its influence on mechanochemical transformations even on cryogrinding, when any fluid water gets frozen.^{4,114-120}

Acknowledgements.

Prof Michael J Pikal passed away on February 26, 2018, which is a major loss for the scientific community. Professor Pikal’s seminal scientific contributions are summarized by Steven Nail.¹²¹ Authors thank Dr. Boris Zakharov for his help with preparation of figures, and Dr. Bakul Bhatnagar for valuable suggestions. JAZ would like to thank the U.K. Engineering and Physical Sciences Research Council (EPSRC), project EP/N022769/1, for funding. Finally, the authors thank anonymous reviewers for valuable inputs and comments.

Figure legends.

Scheme 1. First two steps of deamidation reaction.

Figure 1. DTA cooling (A) and heating (B) curves of sucrose solutions with sucrose concentration 60 , 62.5, and 65 wt% (from the top to the bottom). Panel (C) shows DTA heating curves of 77 wt% sucrose sample. Cooling and heating rates were 0.5 °C/min and 1.5 °C/min, respectively. T_g : the glass transition temperature of the fully amorphous sample; endothermic step, which is marked as T_g' in the Figure, is commonly called T_g'' in the pharmaceutical literature¹²² whereas the food science literature uses T_g' for the same thermal event^{123,124}; T_{AM} thermal event, which was adopted initially from¹²⁵, is called T_g' and T_m' in the contemporary pharmaceutical¹²² and food science^{123,124} literature, respectively. T_D marks water crystallization event. The Y-axis represents the electromotive force of the differential thermocouple; details of the DTA experimental set-up can be found in¹²⁶. The Figure is re-drawn from²⁵.

Figure 2. Mobility modes in solute-water systems. Solid black and blue lines: T_g for sucrose and sorbitol, respectively. Broken line: T_0 for sucrose and water in water-sucrose system from the NMR study.⁴⁰ Red empty squares correspond to the low-temperature T_g in Nafion-water system.¹²⁷ Black squares and blue triangles are for the TSC-detected dipole relaxation event (assigned to be the water glass transition due to rotational mobility) for sucrose and sorbitol, respectively. Red circles at 70 and 100% solute correspond to THz-spectroscopy-detected transition in sorbitol, which was assigned to a conversion from a state with predominantly vibrational modes to a state with rotational degree of freedom.

Figure 3. Limits of crystallization/melting of water in narrow pores showing melting point depression ΔT_m (full symbols) and freezing point depression ΔT_f (open symbols) vs the inverse of the pore radius R_s .⁵⁴ The blue arrow shows the characteristic size of water regions in 70% sorbitol-30% water solution. Reproduced with permission from [Findenegg GH, Jähnert S, Akcakayiran D, Schreiber A 2008. Freezing and melting of water confined in silica nanopores. *ChemPhysChem*. 9(18):2651-2659]. Copyright Willey-VCH Verlag GmbH & Co. KgaA.

Figure 4. (a) (Top, left) Simulation box showing sorbitol matrix for 70% sorbitol-water sample. The arrow shows an example of a void in the sorbitol matrix; the voids are filled by water molecules (water molecules are not shown). (b) (Top, right) Water volume surface contour plot at 100 K showing the regions occupied by water molecules in the sorbitol-water solution. (c) (Bottom) Water volume distribution function for 70 wt% sorbitol-water solution.²²

Figure 5. (a) OW-OW radial distribution functions for 70 wt % sorbitol-water solution (black)²², pure bulk water (green), and water confined in MCM-41 (red) at 298 K.²¹ The OW-OW $g(r)$ for hexagonal ice at 258 K is also shown (blue). The first peak corresponds to the first coordination sphere, second peak to second coordination sphere, etc. (b) Temperature dependence of the full width at half-maximum (FWHM) for the first peak in OW-OW $g(r)$ in hexagonal ice, low-density amorphous water (LDA), bulk water, 70% sorbitol-water, and water confined in MCM-41.²²

Figure 6. (a) Oxygen–oxygen water–water $g(r)$ for 70 wt % sorbitol–water solution at four temperatures. (b) Magnified portions of the $g(r)$ s from Fig. 6a around the second peak. Bottom (c): Comparison of the OW-OW $g(r)$ in the region of the second peak for 70 wt% sorbitol–water (solid lines) and water in MCM41 (dashed lines) at different temperatures.

Figure 7. (a) OW–OW–OW triangles distribution for 70 wt % sorbitol–water solution at four temperatures. To obtain the distribution, the cutoff OW–OW distance is set to 3.20 Å, which corresponds to the position of the first minimum in the OW–OW $g(r)$ ²² (b) Temperature dependence of the water tetrahedrality parameter q in 70 wt % sorbitol–water (black squares²²), MCM41–water (blue rhombs²¹), and bulk water (green circle²¹). Vertical red dotted lines show various characteristic temperatures as follows: T_g of the 70 wt % sorbitol (202 K); terahertz absorption transition (approximately 230 K)⁴⁵; estimate of the break in the Stokes–Einstein relationship for water diffusion.²² The tetrahedral water structure is illustrated in the onset (re-drawn from http://www1.lsbu.ac.uk/water/water_hydrogen_bonding.html).¹²⁸

Figure 8. Experimental rate constants normalized to zero water content for lyophiles (red solid symbols/solid lines), solutions (blue open symbols/ dashed lines), and theoretical estimates for mobility-control chemical reaction in glasses (black stars / dotted lines). Solid squares: amide hydrolysis in freeze-dried Zoniporide.³⁸ Solid inverse triangles: degradation of freeze-dried cefovecin.⁷³ Solid spheres: amide hydrolysis in freeze-dried Zoniporide with 5% sorbitol.³⁸ Solid triangle: deamidation of freeze-dried MAB.¹⁰⁹ Open squares: solvolysis of t-BuCl.¹²⁹ Open spheres: water-catalyzed hydrolysis of [(p-nitrophenyl)sulfonyl]methyl Perchlorate in 1,3-dioxane-water.¹³⁰ Open triangles: acid hydrolysis of acetamide in dioxane-water.¹³¹ Dashed thick line (no symbols): interpolation of the data for unimolecular nucleophilic substitution for t-BuBr.¹³² Open and solid stars: theoretical estimates for mobility-control chemical reaction in glasses for strong and fragile glass-former, respectively.⁷⁰

Figure 9. Schematics of water distribution in trehalose¹³³ (top) and ionophore membrane¹³⁴ (bottom). The top Figure is reprinted with permission from [Lerbret A, Affouard F, Hédoux A, Krenzlin S, Siepmann J, Bellissent-Funel M-C, Descamps M 2012. How strongly does trehalose interact with lysozyme in the solid state? Insights from molecular dynamics simulation and inelastic neutron scattering. *J Phys Chem B*. 116(36):11103-11116]. Copyright 2012 American Chemical Society. The bottom Figure is reprinted with permission from [Li Y, Nguyen QT, Fatyeyeva K, Marais S 2014. Water sorption behavior in different aromatic ionomer composites analyzed with a "New Dual-Mode Sorption" model. *Macromol*. 47(18):6331-6342]. Copyright 2014 American Chemical Society

Figure 10. Impact of water on the Asp-isoAsp conversion in a freeze-dried mAb formulation. The graphs are prepared using data from Breen et al.¹¹⁰ The lines represent fit of the experimental data to the equation below.⁷⁴ The T_g value for the formulation at 5% water content is approx. 40 °C, and therefore the acceleration of the reaction at 8% water could also be associated with the glass transition, as indeed was suggested in the original paper.

$$k/k_0 = \begin{cases} 1 & \text{when } W < W_{sat} \\ 1 + C'_w(W - W_{sat}) & \text{when } W \geq W_{sat} \end{cases}$$

References

1. Hancock BC, Zografi G. Characteristics and significance of the amorphous state in pharmaceutical systems. *J Pharm Sci.* 1997;86(1):1-12.
2. Levine H, Slade L. Water as a plasticizer: physico-chemical aspects of low-moisture polymeric systems. In: Franks F, ed. *Water Science Reviews 3: Water Dynamics*, Cambridge: Cambridge University Press; 1988:79-185.
3. Franks F. Phase changes and chemical reactions in solid aqueous solutions: Science and technology. *Pure Appl Chem.* 1997;69(5):915-920.
4. Rams-Baron M, Jachowicz R, Boldyreva E, Zhou D, Jamroz W, Paluch M. Amorphous Drug Preparation Methods. In: *Amorphous Drugs: Benefits and Challenges*, Cham: Springer International Publishing; 2018:69-106.
5. Bhattacharya S, Suryanarayanan R. Molecular motions in sucrose-PVP and sucrose-sorbitol dispersions: I. Implications of global and local mobility on stability. *Pharm Res.* 2011;28(9):2191-2203.
6. Johari GP, Kim S, Shanker RM. Dielectric study of equimolar acetaminophen-aspirin, acetaminophen-quinidine, and benzoic acid-progesterone molecular alloys in the glass and ultraviscous states and their relevance to solubility and stability. *J Pharm Sci.* 2010;99(3):1358-1374.
7. Cicerone MT, Soles CL. Fast dynamics and stabilization of proteins: Binary glasses of trehalose and glycerol. *Biophys J.* 2004;86(6):3836-3845.
8. Cicerone MT, Douglas JF. β -Relaxation governs protein stability in sugar-glass matrices. *Soft Matter.* 2012;8(10):2983-2991.
9. Ruggiero MT, Krynski M, Kissi EO, Sibik J, Markl D, Tan NY, Arslanov D, van der Zande W, Redlich B, Korter TM, Grohganz H, Lobmann K, Rades T, Elliott SR, Zeitler JA. The significance of the amorphous potential energy landscape for dictating glassy dynamics and driving solid-state crystallisation. *Phys Chem Chem Phys.* 2017;19(44):30039-30047.
10. Levine H, Shalaev EY, Zografi G. The concept of 'structure' in amorphous solids from the perspective of the pharmaceutical sciences. In: Levine H, ed. *Amorphous Food and Pharmaceutical Systems*, Cambridge: The Royal Society of Chemistry; 2002:11-30.
11. Bates S, Zografi G, Engers D, Morris K, Crowley K, Newman A. Analysis of amorphous and nanocrystalline solids from their X-ray diffraction patterns. *Pharm Res.* 2006;23(10):2333-2349.
12. Newman A, Engers D, Bates S, Ivanisevic I, Kelly RC, Zografi G. Characterization of amorphous API:Polymer mixtures using X-ray powder diffraction. *J Pharm Sci.* 2008;97(11):4840-4856.
13. Yu L. Amorphous pharmaceutical solids: preparation, characterization and stabilization. *Adv Drug Deliv Rev.* 2001;48(1):27-42.
14. Zografi G, Newman A. Interrelationships between structure and the properties of amorphous solids of pharmaceutical interest. *J Pharm Sci.* 2017;106(1):5-27.
15. Adam G, Gibbs JH. On the temperature dependence of cooperative relaxation properties in glass-forming liquids. *J Chem Phys.* 1965;43(1):139-146.
16. Ngai KL. Breakdown of Debye-Stokes-Einstein and Stokes-Einstein relations in glass-forming liquids: An explanation from the coupling model. *Philos Mag B.* 1999;79(11-12):1783-1797.
17. Champion D, Hervet H, Blond G, Le Meste M, Simatos D. Translational diffusion in sucrose solutions in the vicinity of their glass transition temperature. *J Phys Chem B.* 1997;101(50):10674-10679.
18. Longinotti MP, Corti HR. Diffusion of ferrocene methanol in super-cooled aqueous solutions using cylindrical microelectrodes. *Electrochem Commun.* 2007;9(7):1444-1450.
19. Corti HR, Frank GA, Marconi MC. Diffusion-viscosity decoupling in supercooled aqueous trehalose solutions. *J Phys Chem B.* 2008;112(41):12899-12906.
20. Parker R, Ring SG. Diffusion in maltose-water mixtures at temperatures close to the glass transition. *Carbohydr Res.* 1995;273(2):147-155.
21. Soper AK. Radical re-appraisal of water structure in hydrophilic confinement. *Chem Phys Lett.* 2013;590(Supplement C):1-15.

22. Shalaev E, Soper AK. Water in a soft confinement: structure of water in amorphous sorbitol. *J Phys Chem B*. 2016;120(29):7289-7296.
23. Franks F. Scientific and technological aspects of aqueous glasses. *Biophys Chem*. 2003;105(2-3):251-261.
24. Corti HR, Angell CA, Auffret T, Levine H, Buera MP, Reid DS, Roos Y, Slade L. Empirical and theoretical models of equilibrium and non-equilibrium transition temperatures of supplemented phase diagrams in aqueous systems (IUPAC Technical Report). *Pure Appl Chem*. 2010;82(5):1065-1097.
25. Shalaev EY. Phase transitions in biopreparations: implications for freeze-drying, PhD Thesis, Koltsovo, Russia: State Research Center of Virology and Biotechnology VECTOR / Institute of Molecular Biology; 1991.
26. Ewing S, Hussain A, Collins G, Roberts C, Shalaev E. Low-temperature mobility of water in sugar glasses: Insights from thermally stimulated current study. In: Gutiérrez-López GF, Alamilla-Beltrán L, del Pilar Buera M, Welti-Chanes J, Parada-Arias E, Barbosa-Cánovas GV, eds. *Water Stress in Biological, Chemical, Pharmaceutical and Food Systems*, New York, NY: Springer New York; 2015:75-87.
27. Rasmussen DH, Luyet B. Complementary study of some non-equilibrium phase transitions in frozen solutions of glycerol, ethylene glycol, glucose and sucrose. *Biodynamica*. 1969;10(220):319-331.
28. MacKenzie AP, Rasmussen DH. Interactions in the water-polyvinylpyrrolidone system at low temperatures. In: Jellinek HHG, ed. *Water Structure at the Water-Polymer Interface*, Boston, MA: Springer US; 1972:146-172.
29. Franks F, Asquith MH, Hammond CC, Skaer HIB, Echlin P. Polymeric cryoprotectants in the preservation of biological ultrastructure. *J Microsc*. 1977;110(3):223-238.
30. Roos YH, Potes N. Quantification of protein hydration, glass transitions, and structural relaxations of aqueous protein and carbohydrate-protein systems. *J Phys Chem B*. 2015;119(23):7077-7086.
31. Franks F. Unfrozen water: yes; unfreezable water: hardly; bound water: certainly not. *Cryo-Letters*. 1986;7:207-211.
32. Shalaev EY, Franks F. Structural glass transitions and thermophysical processes in amorphous carbohydrates and their supersaturated solutions. *J Chem Soc, Faraday Trans*. 1995;91(10):1511-1517.
33. Bhattacharya S, Suryanarayanan R. Local mobility in amorphous pharmaceuticals--characterization and implications on stability. *J Pharm Sci*. 2009;98(9):2935-2953.
34. Andronis V, Zografi G. Crystal nucleation and growth of indomethacin polymorphs from the amorphous state. *J Non-Cryst Solids*. 2000;271(3):236-248.
35. Shalaev EY, Zografi G, Steponkus PL. Occurrence of glass transitions in long-chain phosphatidylcholine mesophases. *J Phys Chem B*. 2010;114(10):3526-3533.
36. Hans Tromp R, Parker R, Ring SG. Water diffusion in glasses of carbohydrates. *Carbohydr Res*. 1997;303(2):199-205.
37. Zhu L, Cai T, Huang J, Stringfellow TC, Wall M, Yu L. Water self-diffusion in glassy and liquid maltose measured by Raman microscopy and NMR. *J Phys Chem B*. 2011;115(19):5849-5855.
38. Luthra SA, Shalaev EY, Medek A, Hong J, Pikal MJ. Chemical stability of amorphous materials: specific and general media effects in the role of water in the degradation of freeze-dried zoniporide. *J Pharm Sci*. 2012;101(9):3110-3123.
39. Rodríguez O, Fomasiero F, Arcea A, Radkea CJ, Prausnitz JM. Solubilities and diffusivities of water vapor in poly(methylmethacrylate), poly(2-hydroxyethylmethacrylate), poly(N-vinyl-2-pyrrolidone) and poly(acrylonitrile). *Polymer*. 2003;44(20):6323-6333.
40. Girlich D, Lüdemann HD. Molecular mobility of the water molecules in aqueous sucrose solutions, studied by 2H-NMR relaxation. *Z Naturforsch C Biosci*. 1994;49(3-4):250-257.

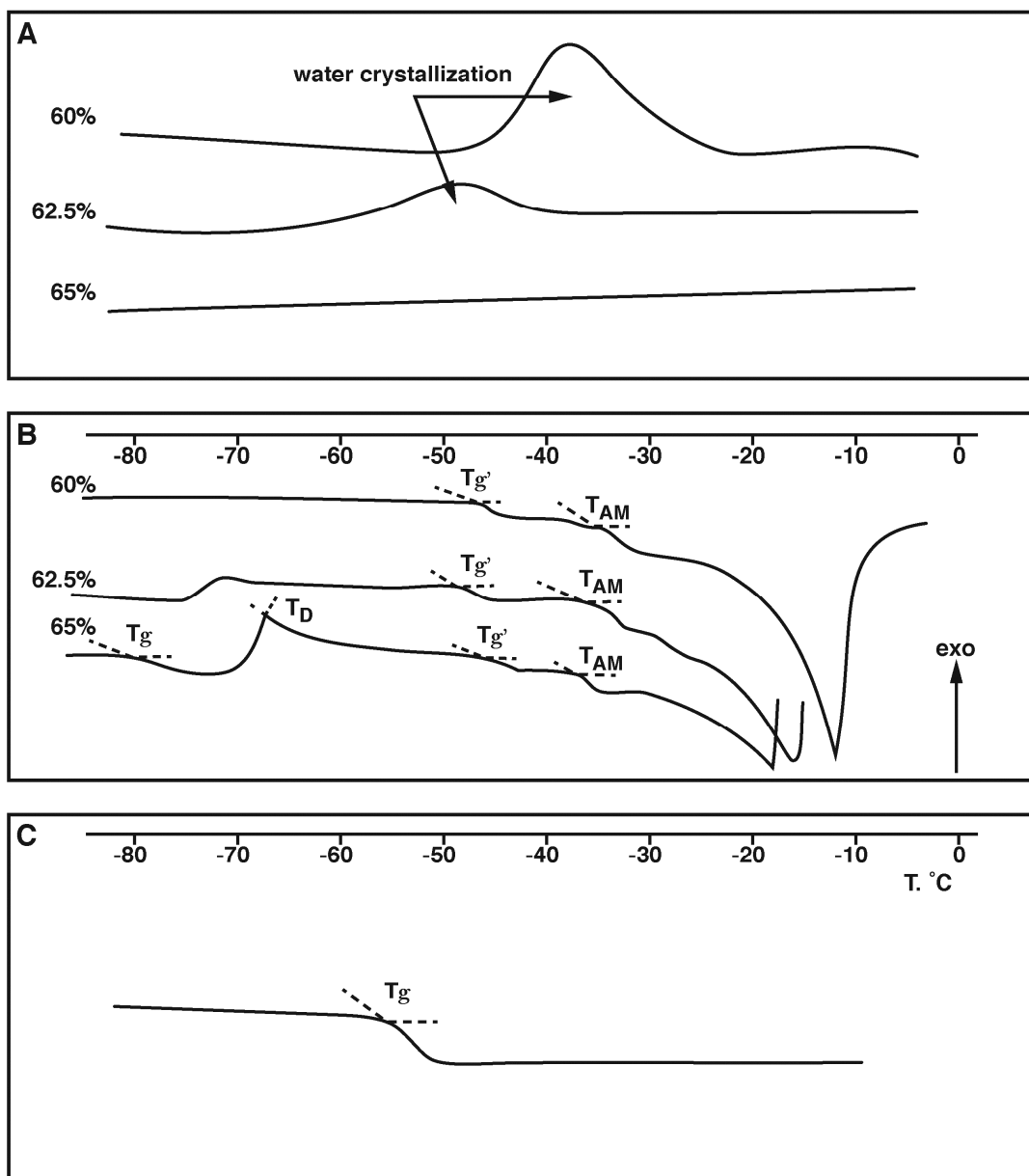
41. Johari GP, Hallbrucker A, Mayer E. The glass–liquid transition of hyperquenched water. *Nature*. 1987;330:552-553.
42. Mayer E. Calorimetric glass transitions in the amorphous forms of water: a comparison. *J Mol Struct*. 1991;250(2):403-411.
43. Handa YP, Klug DD. Heat capacity and glass transition behavior of amorphous ice. *J Phys Chem*. 1988;92(12):3323-3325.
44. Sugisaki M, Suga H, Seki S. Calorimetric study of glassy state. V. Heat capacities of glassy water and cubic ice. *Bull Chem Soc Jpn*. 1968;41:2591-2599.
45. Sibik J, Shalaev EY, Zeitler JA. Glassy dynamics of sorbitol solutions at terahertz frequencies. *Phys Chem Chem Phys*. 2013;15(28):11931-11942.
46. Pikal MJ, Shah S, Roy ML, Putman R. The secondary drying stage of freeze drying: drying kinetics as a function of temperature and chamber pressure. *Int J Pharm*. 1990;60(3):203-207.
47. Taylor LS, Langkilde FW, Zografi G. Fourier transform Raman spectroscopic study of the interaction of water vapor with amorphous polymers. *J Pharm Sci*. 2001;90(7):888-901.
48. Patel SM, Doen T, Pikal MJ. Determination of end point of primary drying in freeze-drying process control. *AAPS PharmSciTech*. 2010;11(1):73-84.
49. Petrenko VF, Whitworth RW. *Physics of Ice*. Oxford: University Press; 1999.
50. Varshney DB, Elliott JA, Gatlin LA, Kumar S, Suryanarayanan R, Shalaev EY. Synchrotron X-ray diffraction investigation of the anomalous behavior of ice during freezing of aqueous systems. *J Phys Chem B*. 2009;113(18):6177-6182.
51. Malenkov G. *Liquid water and ices: understanding the structure and physical properties*. J Phys: Condens Matter. 2009;21(28):283101.
52. Rosa M, Lopes C, Melo EP, Singh SK, Geraldes V, Rodrigues MA. Measuring and modeling hemoglobin aggregation below the freezing temperature. *J Phys Chem B*. 2013;117(30):8939-8946.
53. Sartor G, Hallbrucker A, Mayer E. Characterizing the secondary hydration shell on hydrated myoglobin, hemoglobin, and lysozyme powders by its vitrification behavior on cooling and its calorimetric glass-->liquid transition and crystallization behavior on reheating. *Biophys J*. 69(6):2679-2694.
54. Findenegg GH, Jähnert S, Akcakayiran D, Schreiber A. Freezing and melting of water confined in silica nanopores. *ChemPhysChem*. 2008;9(18):2651-2659.
55. Suzuki Y, Duran H, Steinhart M, Kappl M, Butt H-J, Floudas G. Homogeneous nucleation of predominantly cubic ice confined in nanoporous alumina. *Nano Lett*. 2015;15(3):1987-1992.
56. Thanatuksoorn P, Kajiwaru K, Murase N, Franks F. Freeze-thaw behaviour of aqueous glucose solutions--the crystallisation of cubic ice. *Phys Chem Chem Phys*. 2008;10(35):5452-5458.
57. Dowell LG, Moline SW, Rinfret AP. A low-temperature X-ray diffraction study of ice structures formed in aqueous gelatin gels. *Biochimica et Biophysica Acta*. 1962;59(1):158-167.
58. Lowell S, Shields JE, Thomas MA, Thommes M. *Characterization of Porous Solids and Powders: Surface Area, Pore Size and Density*. Dordrecht, The Netherlands: Kluwer Academic Publishers; 2004.
59. Impéror-Clerc M, Davidson P, Davidson A. Existence of a Microporous Corona around the Mesopores of Silica-Based SBA-15 Materials Templated by Triblock Copolymers. *J Am Chem Soc*. 2000;122(48):11925-11933.
60. Solovyov LA, Belousov OV, Dinnebier RE, Shmakov AN, Kirik SD. X-ray diffraction structure analysis of MCM-48 mesoporous silica. *J Phys Chem B*. 2005;109(8):3233-3237.
61. Zickler GA, Jähnert S, Wagermaier W, Funari SS, Findenegg GH, Paris O. Physisorbed films in periodic mesoporous silica studied by in situ synchrotron small-angle diffraction. *Phys Rev B*. 2006;73(18):184109.
62. Shenderovich IG, Buntkowsky G, Schreiber A, Gedat E, Sharif S, Albrecht J, Golubev NS, Findenegg GH, Limbach H-H. Pyridine-15N A Mobile NMR Sensor for Surface Acidity and Surface Defects of Mesoporous Silica. *J Phys Chem B*. 2003;107(43):11924-11939.

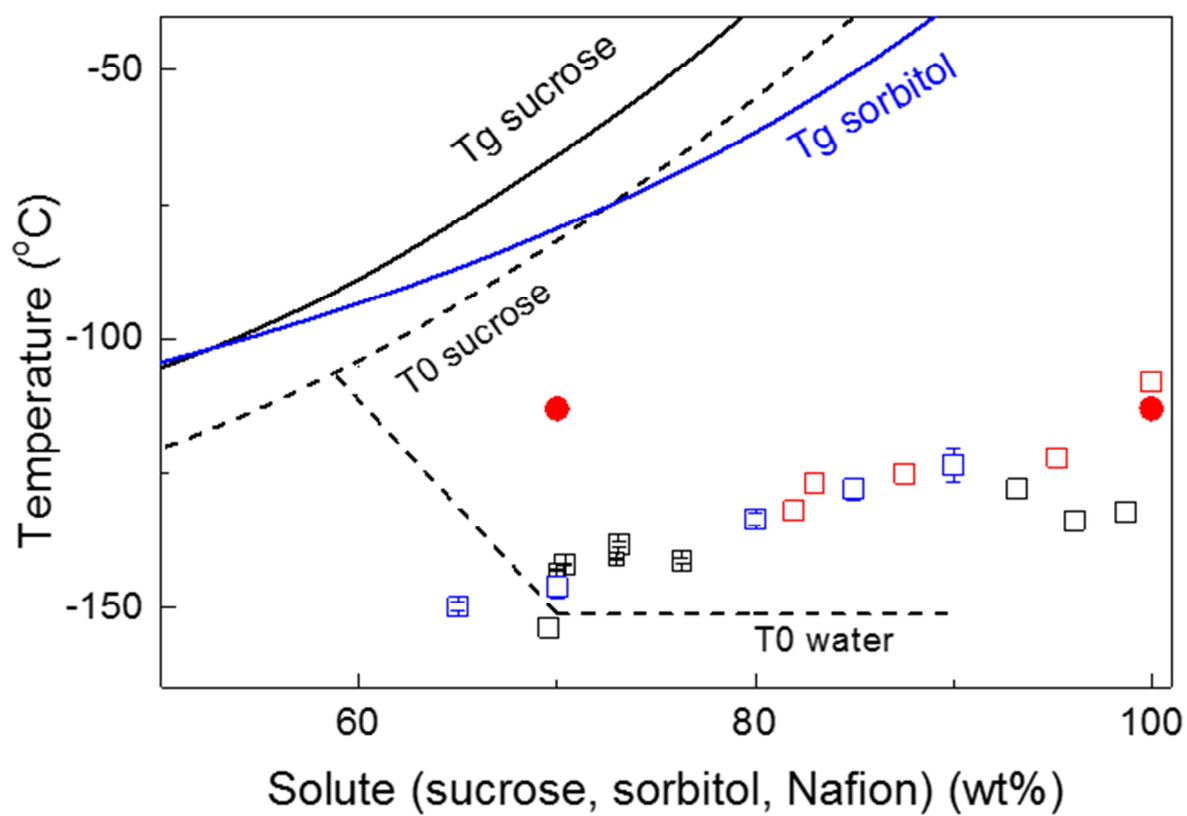
63. Shenderovich IG, Mauder D, Akcakayiran D, Buntkowsky G, Limbach H-H, Findenegg GH. NMR Provides Checklist of Generic Properties for Atomic-Scale Models of Periodic Mesoporous Silicas. *J Phys Chem B*. 2007;111(42):12088-12096.
64. Errington JR, Debenedetti PG. Relationship between structural order and the anomalies of liquid water. *Nature*. 2001;409:318-321.
65. Molinero V, Çağın T, Goddard WA. Mechanisms of nonexponential relaxation in supercooled glucose solutions: the role of water facilitation. *J Phys Chem A*. 2004;108(17):3699-3712.
66. Roberts CJ, Debenedetti PG. Structure and dynamics in concentrated, amorphous carbohydrate–water systems by molecular dynamics simulation. *J Phys Chem B*. 1999;103(34):7308-7318.
67. Towey JJ, Soper AK, Dougan L. Molecular insight into the hydrogen bonding and micro-segregation of a cryoprotectant molecule. *J Phys Chem B*. 2012;116(47):13898-13904.
68. Zhao Z, Angell CA. Apparent first-order liquid-liquid transition with pre-transition density anomaly, in water-rich ideal solutions. *Angew Chem Int Ed Engl*. 2016;55(7):2474-2477.
69. Kanno H, Speedy RJ, Angell CA. Supercooling of water to -92°C under pressure. *Science*. 1975;189(4206):880-881.
70. Shalaev EY, Zografi G. How does residual water affect the solid-state degradation of drugs in the amorphous state? *J Pharm Sci*. 1996;85(11):1137-1141.
71. Abdul-Fattah AM, Dellerman KM, Bogner RH, Pikal MJ. The effect of annealing on the stability of amorphous solids: Chemical stability of freeze-dried moxalactam. *J Pharm Sci*. 2007;96(5):1237-1250.
72. Shamblin SL, Hancock BC, Pikal MJ. Coupling between chemical reactivity and structural relaxation in pharmaceutical glasses. *Pharm Res*. 2006;23(10):2254-2268.
73. Ohtake S, Shalaev E. Effect of water on the chemical stability of amorphous pharmaceuticals: I. Small molecules. *J Pharm Sci*. 2013;102(4):1139-1154.
74. Ohtake S, Feng S, Shalaev E. Effect of water on the chemical stability of amorphous pharmaceuticals: 2. Deamidation of peptides and proteins. *J Pharm Sci*. 2017;107(1):42-56.
75. Hill JJ, Shalaev EY, Zografi G. Thermodynamic and dynamic factors involved in the stability of native protein structure in amorphous solids in relation to levels of hydration. *J Pharm Sci*. 2005;94(8):1636-1667.
76. Luthra SA, Hodge IM, Utz M, Pikal MJ. Correlation of annealing with chemical stability in lyophilized pharmaceutical glasses. *J Pharm Sci*. 2008;97(12):5240-5251.
77. Chang C-R, Huang Z-Q, Li J. The promotional role of water in heterogeneous catalysis: mechanism insights from computational modeling. *Wiley Interdiscip Rev Comput Mol Sci*. 2016;6(6):679-693.
78. Catak S, Monard G, Aviyente V, Ruiz-López MF. Reaction mechanism of deamidation of asparaginyl residues in peptides: Effect of solvent molecules. *J Phys Chem A*. 2006;110(27):8354-8365.
79. Catak S, Monard G, Aviyente V, Ruiz-López MF. Deamidation of asparagine residues: Direct hydrolysis versus succinimide-mediated deamidation mechanisms. *J Phys Chem A*. 2009;113(6):1111-1120.
80. Kaliman I, Nemukhin A, Varfolomeev S. Free energy barriers for the N-terminal asparagine to succinimide conversion: Quantum molecular dynamics simulations for the fully solvated model. *J Chem Theory Comput*. 2010;6(1):184-189.
81. Halim MA, Almatarneh MH, Poirier RA. Mechanistic study of the deamidation reaction of glutamine: A computational approach. *J Phys Chem B*. 2014;118(9):2316-2330.
82. Takahashi O, Kirikoshi R, Manabe N. Roles of intramolecular and intermolecular hydrogen bonding in a three-water-assisted mechanism of succinimide formation from aspartic acid residues. *Molecules*. 2014;19(8):11440-11452.
83. Zahn D. Theoretical study of the mechanisms of acid-catalyzed amide hydrolysis in aqueous solution. *J Phys Chem B*. 2003;107(44):12303-12306.

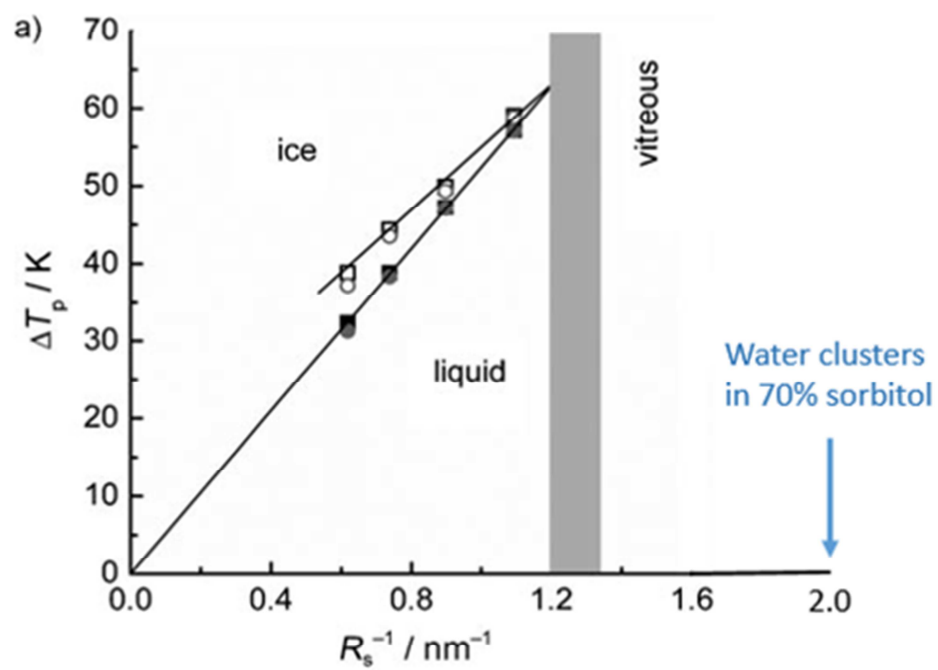
84. Ribe S, Wipf P. Water-accelerated organic transformations. *Chem Commun.* 2001(4):299-307.
85. Govindarajan R, Chatterjee K, Gatlin L, Suryanarayanan R, Shalaev EY. Impact of freeze-drying on ionization of sulfonephthalein probe molecules in trehalose-citrate systems. *J Pharm Sci.* 2006;95(7):1498-1510.
86. Agmon N. Hydrogen bonds, water rotation and proton mobility. *J Chim Phys.* 1996;93:1714-1736.
87. Li Y, Williams TD, Topp EM. Effects of excipients on protein conformation in lyophilized solids by hydrogen/deuterium exchange mass spectrometry. *Pharm Res.* 2008;25(2):259-267.
88. Li Y, Williams TD, Schowen RL, Topp EM. Characterizing protein structure in amorphous solids using hydrogen/deuterium exchange with mass spectrometry. *Anal Biochem.* 2007;366(1):18-28.
89. Moorthy BS, Zarraga IE, Kumar L, Walters BT, Goldbach P, Topp EM, Allmendinger A. Solid-state Hydrogen–Deuterium exchange mass spectrometry: Correlation of Deuterium uptake and long-term stability of lyophilized monoclonal antibody formulations. *Mol Pharm.* 2018;15(1):1-11.
90. Pogocki D, Ghezzi-Schöneich E, Schöneich C. Conformational flexibility controls proton transfer between the methionine hydroxy sulfuranyl radical and the N-terminal amino group in Thr-(X)_n-Met peptides. *J Phys Chem B.* 2001;105(6):1250-1259.
91. Eikerling M, Kornyshev AA, Spohr E. Proton-conducting polymer electrolyte membranes: Water and structure in charge. In: Scherer GG, ed. *Advances in Polymer Science: Fuel Cells I*, Berlin, Heidelberg: Springer Berlin Heidelberg; 2008:15-54.
92. Marx D, Tuckerman ME, Hutter J, Parrinello M. The nature of the hydrated excess proton in water. *Nature.* 1999;397:601-604.
93. Cukierman S. Et tu, Grotthuss! and other unfinished stories. *BBA-Bioenergetics.* 2006;1757(8):876-885.
94. Roscioli JR, McCunn LR, Johnson MA. Quantum structure of the intermolecular proton bond. *Science.* 2007;316(5822):249-254.
95. Eigen M. Proton transfer, acid-base catalysis, and enzymatic hydrolysis. Part I: elementary processes. *Angew Chem Int Ed Engl.* 1964;3(1):1-19.
96. Devlin JP, Buch V, Mohamed F, Parrinello M. The amorphous analogs of the crystalline monohydrate of HCl: Structures and spectra. *Chem Phys Lett.* 2006;432(4):462-467.
97. Ortega IK, Escribano R, Herrero VJ, Maté B, Moreno MA. The structure and vibrational frequencies of crystalline HCl trihydrate. *J Mol Struct.* 2005;742(1):147-152.
98. Hayes RL, Paddison SJ, Tuckerman ME. Proton transport in triflic acid pentahydrate studied via ab initio path integral molecular dynamics. *J Phys Chem A.* 2011;115(23):6112-6124.
99. Xiang TX, Anderson BD. Distribution and effect of water content on molecular mobility in poly(vinylpyrrolidone) glasses: A molecular dynamics simulation. *Pharm Res.* 2005;22(8):1205-1214.
100. Zimm BH. Simplified relation between thermodynamics and molecular distribution functions for a mixture. *J Chem Phys.* 1953;21(5):934-935.
101. Zimm BH, Lundberg JL. Sorption of vapors by high polymers. *J Phys Chem A.* 1956;60(4):425-428.
102. Starkweather HW. Clustering of water in polymers. *J Polym Sci, Part B: Polym Lett.* 1963;1(3):133-138.
103. Authelin JR, MacKenzie AP, Rasmussen DH, Shalaev EY. Water clusters in amorphous pharmaceuticals. *J Pharm Sci.* 2014;103(9):2663-2672.
104. Authelin JR. Unpublished data, the method is described in Ref 105.
105. Authelin J-R. Thermodynamics of non-stoichiometric pharmaceutical hydrates. *Int J Pharm.* 2005;303(1):37-53.
106. Peng C, Chan CK, Chow AHL. Hygroscopic study of glucose, citric acid, and sorbitol using an electrodynamic balance: Comparison with UNIFAC predictions. *Aerosol Sci Technol.* 2001;35(3):753-758.
107. Donghun K, Sien-Ho H, C.S.P. S. Characterization of water in perfluorosulfonic acid polymer (Nafion) by near-IR and pressure DSC studies. *Polym Mater Sci Eng.* 2005;93:465-467.

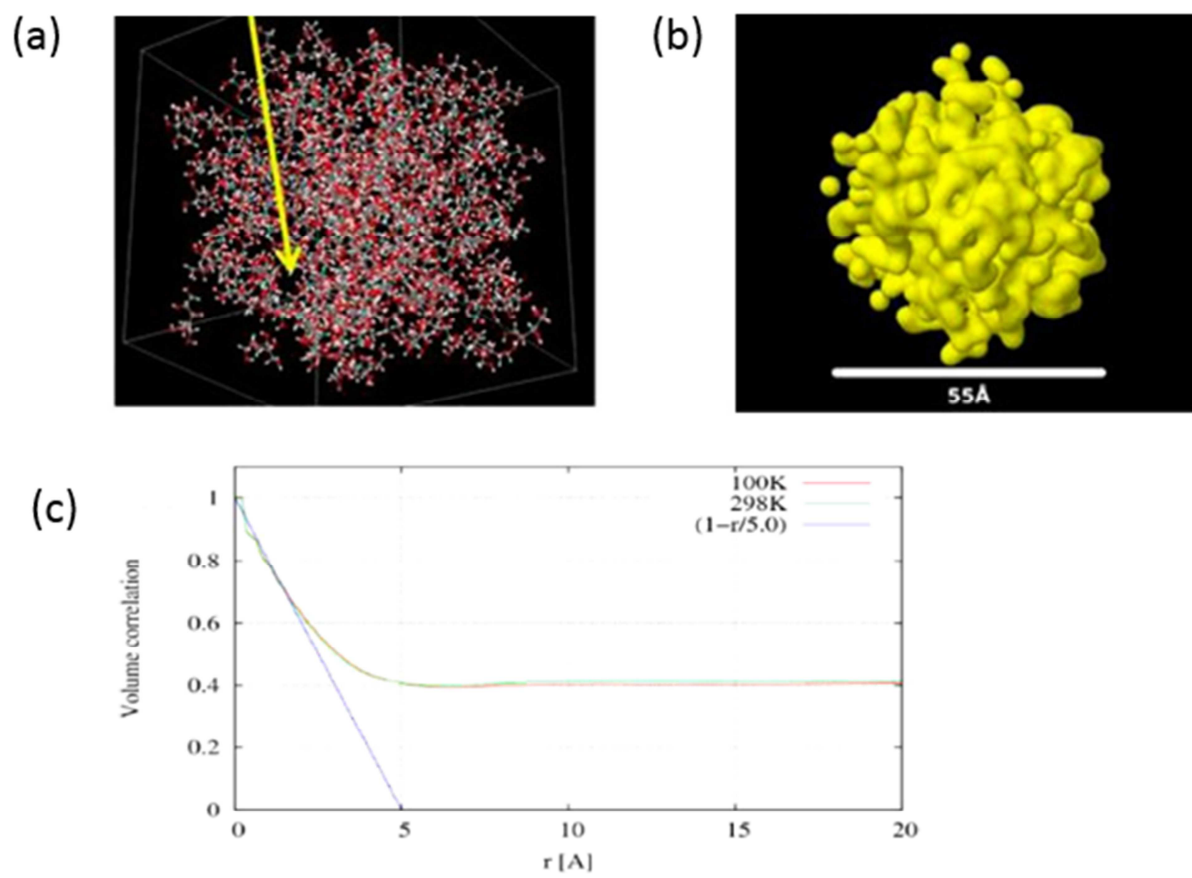
108. Pikal MJ, Rigsbee DR. The Stability of Insulin in Crystalline and Amorphous Solids: Observation of Greater Stability for the Amorphous Form. *Pharm Res.* 1997;14(10):1379-1387.
109. Chang LL, Shepherd D, Sun J, Tang XC, Pikal MJ. Effect of sorbitol and residual moisture on the stability of lyophilized antibodies: Implications for the mechanism of protein stabilization in the solid state. *J Pharm Sci.* 2005;94(7):1445-1455.
110. Breen ED, Curley JG, Overcashier DE, Hsu CC, Shire SJ. Effect of moisture on the stability of a lyophilized humanized monoclonal antibody formulation. *Pharm Res.* 2001;18(9):1345-1353.
111. Dzyuba SA, Tsvetkov YD. Molecular motion in supercooled liquids and glasses. *J Struct Chem.* 1987;28(3):343-363.
112. Moussa EM, Singh SK, Kimmel M, Nema S, Topp EM. Probing the conformation of an IgG1 monoclonal antibody in lyophilized solids using solid-state Hydrogen–Deuterium exchange with mass spectrometric analysis (ssHDX-MS). *Mol Pharm.* 2018;15(2):356-368.
113. Mensink MA, Sibik J, Frijlink HW, van der Voort Maarschalk K, Hinrichs WLJ, Zeitler JA. Thermal gradient mid- and far-infrared spectroscopy as tools for characterization of protein carbohydrate lyophilizates. *Mol Pharm.* 2017;14(10):3550-3557.
114. Hasa D, Rauber GS, Voinovich D, Jones W. Cocrystal Formation through Mechanochemistry: from Neat and Liquid-Assisted Grinding to Polymer-Assisted Grinding. *Angew Chem Int Ed Engl.* 2015;54(25):7371-7375.
115. Tumanov IA, Michalchuk AAL, Politov AA, Boldyreva EV, Boldyrev VV. Inhibition of organic mechanochemical synthesis by water vapor. *Dokl Chem.* 2017;472(1):17-19.
116. Tumanov IA, Michalchuk AAL, Politov AA, Boldyreva EV, Boldyrev VV. Inadvertent liquid assisted grinding: a key to "dry" organic mechano-co-crystallisation? *CrystEngComm.* 2017;19(21):2830-2835.
117. Boldyreva E. Non-ambient conditions in the investigation and manufacturing of drug forms. *Curr Pharm Des.* 2016;22(32):4981-5000.
118. Boldyreva E. Mechanochemistry of inorganic and organic systems: what is similar, what is different? *Chem Soc Rev.* 2013;42(18):7719-7738.
119. Kosova NV, Khabibullin AK, Boldyrev VV. Hydrothermal reactions under mechanochemical treating. *Solid State Ionics.* 1997;101-103:53-58.
120. Belenguer AM, Lampronti GI, Cruz-Cabeza AJ, Hunter CA, Sanders JKM. Solvation and surface effects on polymorph stabilities at the nanoscale. *Chem Sci.* 2016;7(11):6617-6627.
121. Nail S. Professor Michael J. Pikal: Scientist, family man, educator, colleague and friend. *J Pharm Sci.* 2009;98(9):2869-2874.
122. Tang XC, Pikal MJ. Design of Freeze-Drying Processes for Pharmaceuticals: Practical Advice. *Pharm Res.* 2004;21(2):191-200.
123. Harnkarnsujarit N, Charoenrein S, Roos YH. Microstructure formation of maltodextrin and sugar matrices in freeze-dried systems. *Carbohydr Polym.* 2012;88(2):734-742.
124. Roos YH. Melting and glass transitions of low molecular weight carbohydrates. *Carbohydr Res.* 1993;238:39-48.
125. Luyet B, Rasmussen D. Study by differential thermal analysis of the temperatures of instability of rapidly cooled solutions of glycerol, ethylene glycol, sucrose and glucose. *Biodynamica.* 1968;10(210):167-191.
126. Shalaev EJ, Malakhov DV, Kanev AN, Kosyakov VI, Tuzikov FV, Varaksin NA, Vavilin VI. Study of the phase diagram water fraction of the system water-glycine-sucrose by DTA and X-ray diffraction methods. *Thermochim Acta.* 1992;196(1):213-220.
127. Corti HR, Nores-Pondal F, Pilar Buera M. Low temperature thermal properties of Nafion 117 membranes in water and methanol-water mixtures. *J Power Sources.* 2006;161(2):799-805.
128. Chaplin M Hydrogen Bonding in Water. Available at: http://www1.lsbu.ac.uk/water/water_hydrogen_bonding.html. Accessed June 2018.
129. Winstein S, Fainberg AH. Correlation of solvolysis rates. IV. Solvent effects on enthalpy and entropy of activation for solvolysis of t-butyl chloride. *J Am Chem Soc.* 1957;79(22):5937-5950.

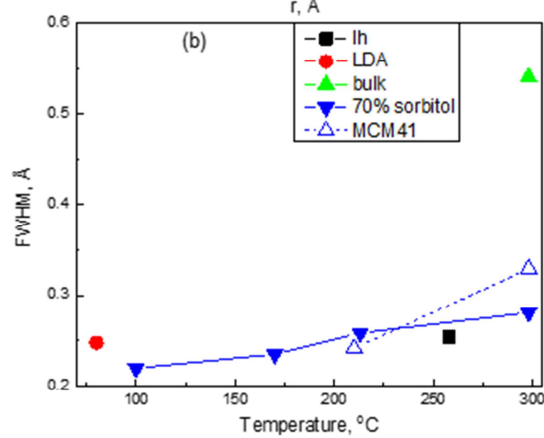
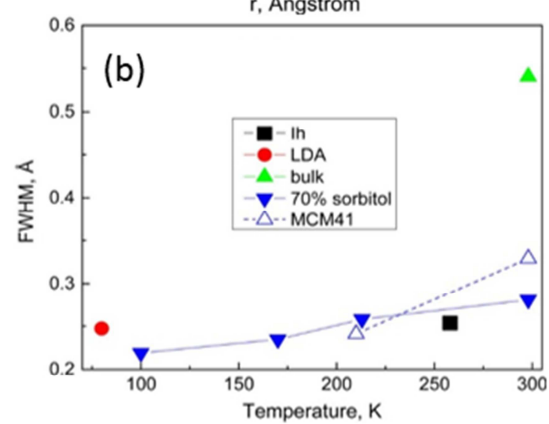
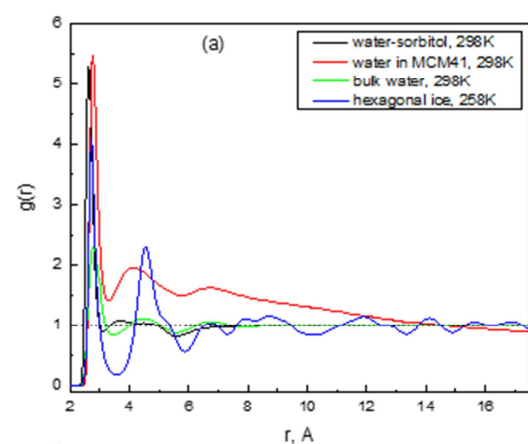
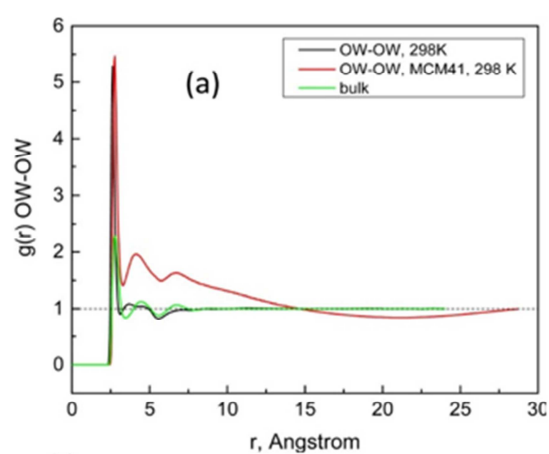
130. Remerie K, Engberts JBFN. Comparative study of the water-catalyzed hydrolysis of [(p-nitrophenyl)sulfonyl]methyl perchlorate in 1,4-dioxane-water and in 1,3-dioxane-water. *J Org Chem.* 1981;46(17):3543-3546.
131. Koskikallio J. Kinetics of the acid hydrolysis of acetamide in dioxan-water mixtures. *Acta Chem Scand.* 1964;18:1831-1838.
132. Ingold CK. *Structure and Mechanism in Organic Chemistry.* 2nd ed, London: Cornell University Press; 1969.
133. Lerbret A, Affouard F, Hédoux A, Krenzlin S, Siepmann J, Bellissent-Funel M-C, Descamps M. How strongly does trehalose interact with lysozyme in the solid state? Insights from molecular dynamics simulation and inelastic neutron scattering. *J Phys Chem B.* 2012;116(36):11103-11116.
134. Li Y, Nguyen QT, Fatyeyeva K, Marais S. Water sorption behavior in different aromatic ionomer composites analyzed with a "New Dual-Mode Sorption" model. *Macromol.* 2014;47(18):6331-6342.

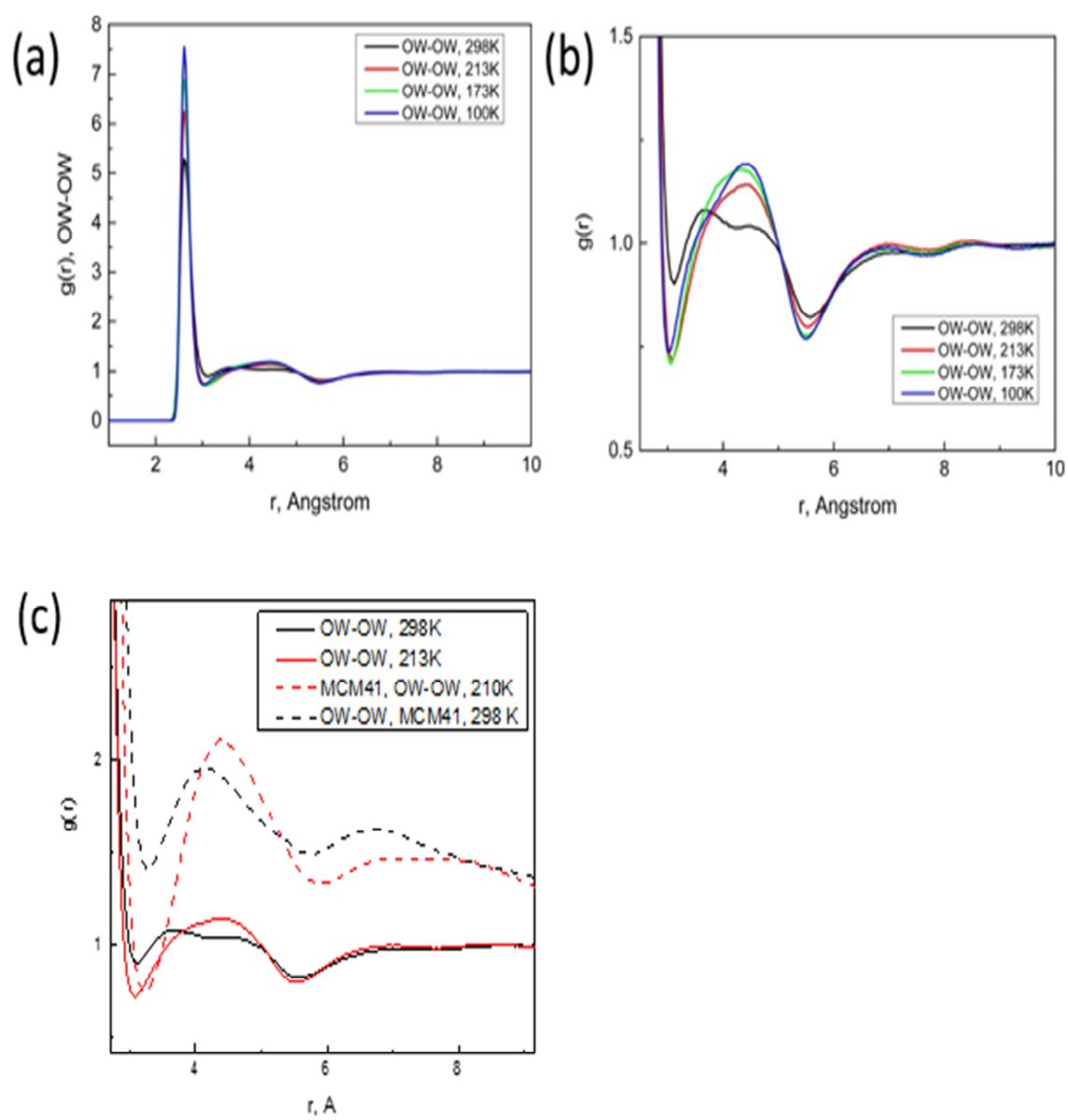


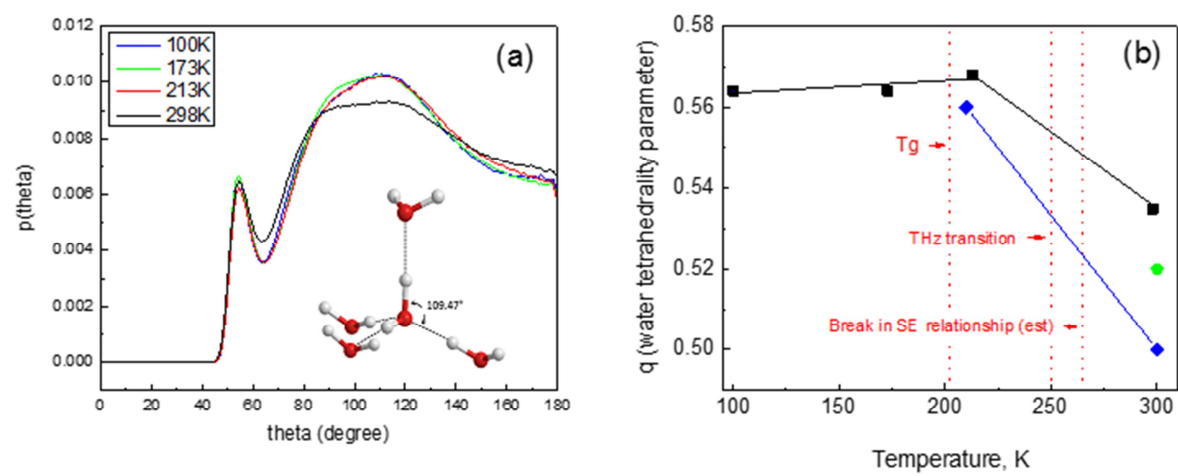


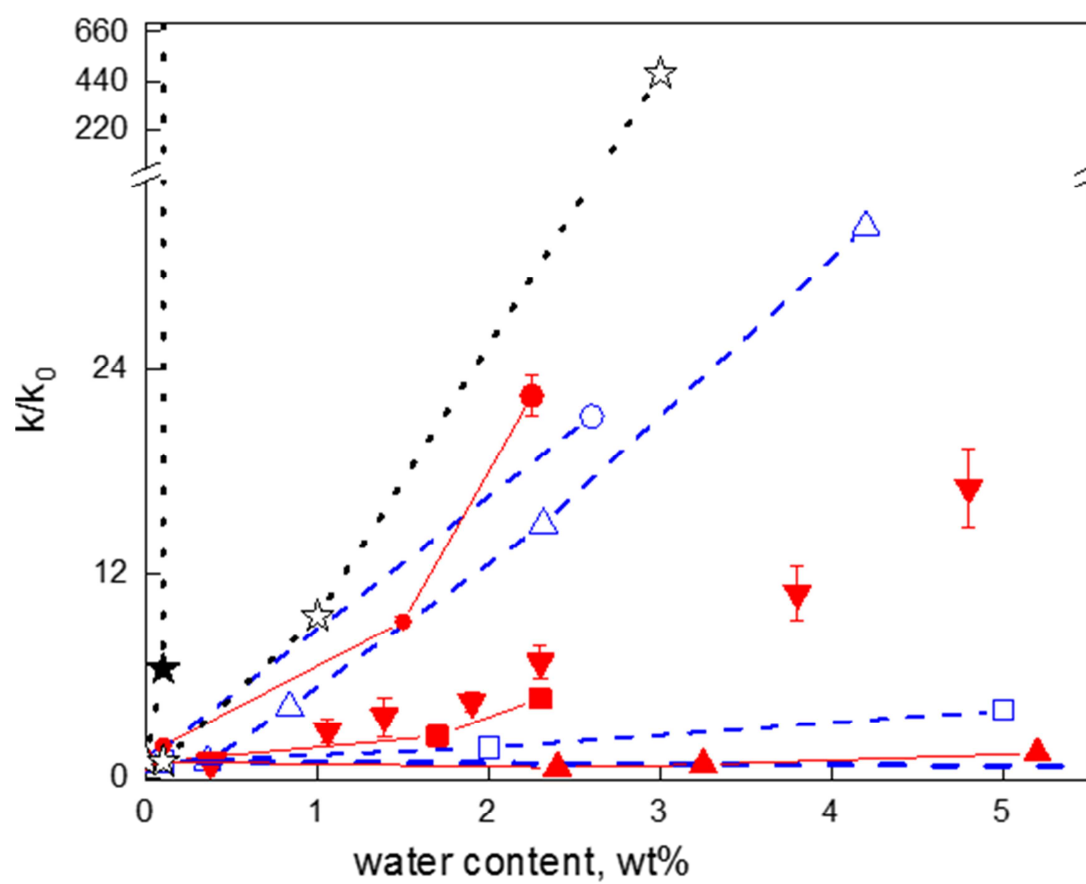


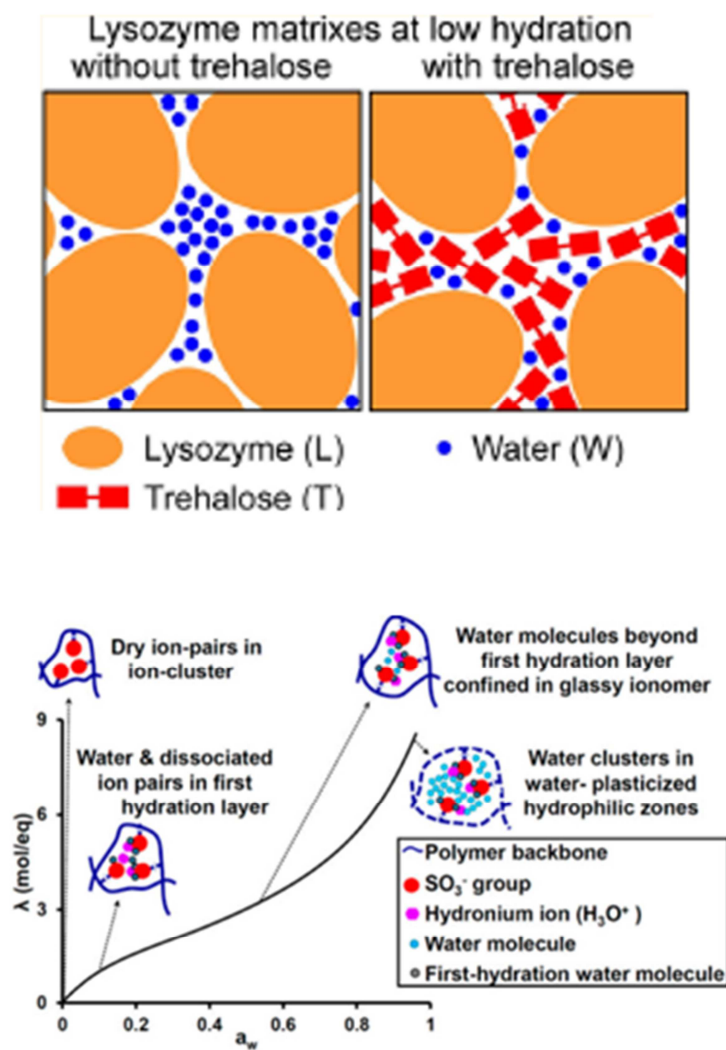


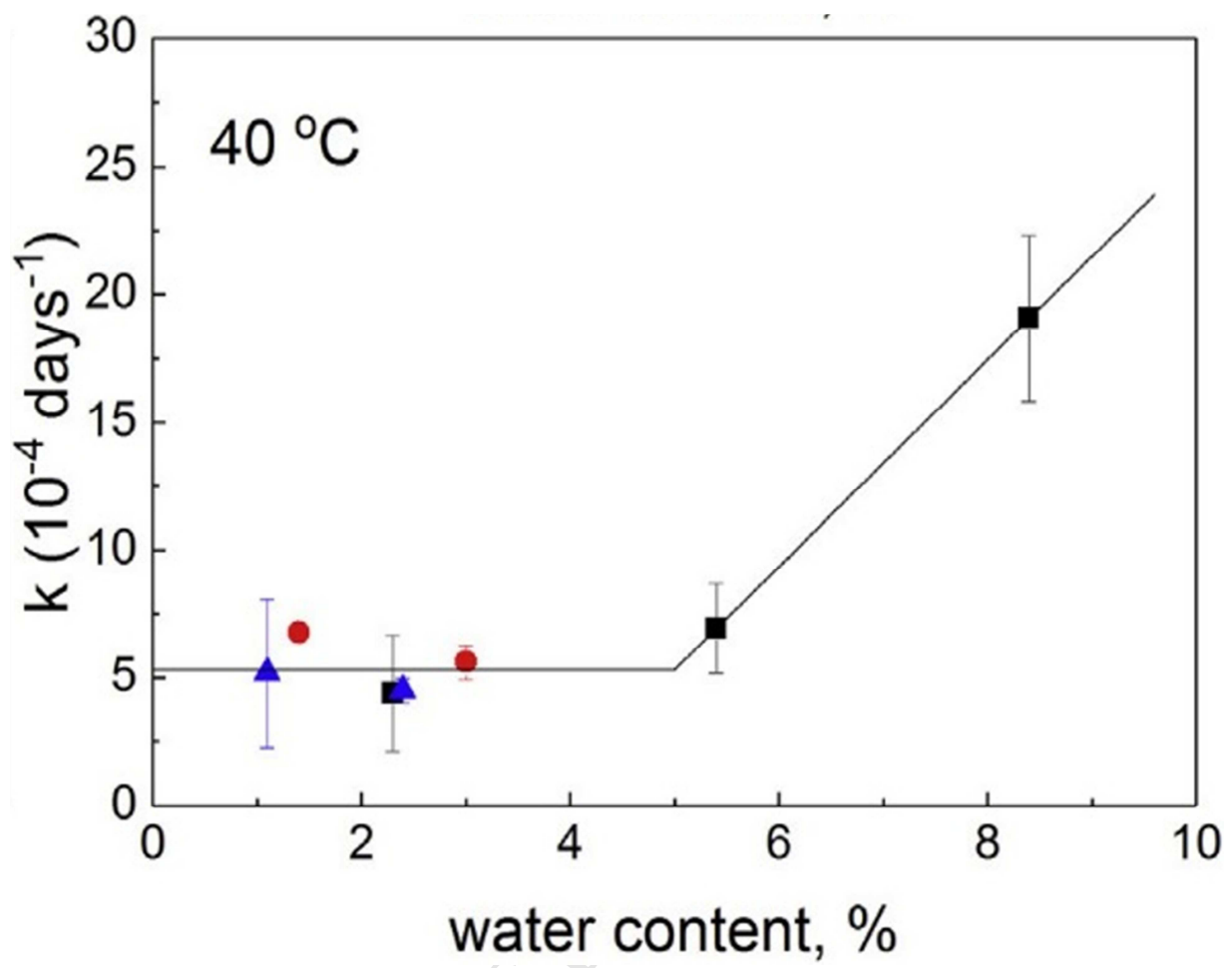


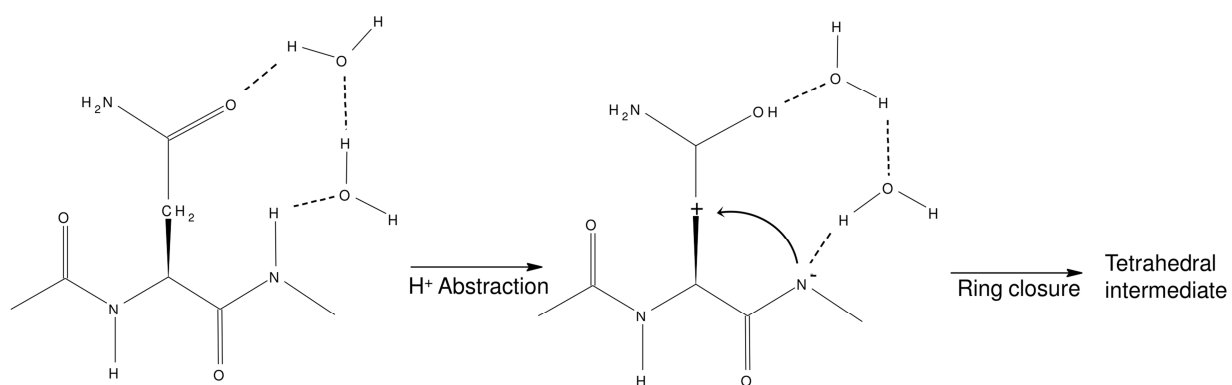












ACCEPTED MANUSCRIPT